Fall 12-2-2010

A COMPREHENSIVE ANALYSIS OF LTE PHYSICAL LAYER

Fahimeh Rezaei
University of Nebraska-Lincoln, fahimeh.rezaei.83@gmail.com

A COMPREHENSIVE ANALYSIS OF LTE PHYSICAL LAYER

by

Fahimeh Rezaei

A THESIS

Presented to the Faculty of

The Graduate College at the University of Nebraska

In Partial Fulfillment of Requirements

For the Degree of Master of Science

Major: Telecommunications Engineering

Under the Supervision of Professor Hamid.R Sharif-Kashani

Lincoln, Nebraska

December, 2010

A COMPREHENSIVE ANALYSIS OF THE LTE PHYSICAL LAYER

Fahimeh Rezaei, M.S.

University of Nebraska, 2010

Advisor: Hamid.R Sharif-Kashani

The 3rd Generation Partnership Project (3GPP) introduced Long Term Evolution (LTE) as the 3rd generation of mobile communication standards. LTE Release 8 describes a mobile communication standard which supports up to 300 Mbps of data transmission in downlink using the OFDM scheme as well as up to 75 Mbps throughput for uplink using the SC-FDMA modulation. In this thesis, an in-depth study of LTE performance based on Release 8 is conducted for uplink and downlink under different scenarios. The main objective of this study is to investigate a comprehensive analysis of physical layer throughput of LTE Release8 based on standard parameters for different channel bandwidths, duplex schemes, antenna diversity and other scenarios. Our study of the FDD operation mode shows that the maximum throughput for downlink data is 299.122 by using 4 antenna ports with the least possible control overhead (one OFDM symbol assigned to PDCCH), 64-QAM data modulation scheme, the maximum code rate (0.92), and the maximum channel bandwidth (20 MHz). This throughput result is based on PDSCH that is used for data transmission only and does not include control information (PDCCH, PHICH, and PCFICH), broadcast channel (PBCH), reference signals, and Synchronization Signals (P-SS and S-SS). Our study also shows that the maximum uplink throughput for the FDD operation is 71.97 Mbps excluding control channel

information (PUCCH), and reference signals (demodulation reference signals and sounding reference signal). This maximum throughput result is based on assuming 64-QAM data modulation, maximum bandwidth (20 MHz), and 0.85 code rate.

This study also presents other throughput results based on different parameters. Overall, this thesis provides a comprehensive investigation of the LTE performance analysis based on detailed physical layer parameters to fill the existing gap in current literature in performance study of LTE.

Table of Contents

List of Figures

List of Tables

Acronyms

3GPP	3rd Generation Partnership Project
AM	Amplitude Modulation
AMPS	Advanced Mobile Phone Service
APN	Access Point Name
BER	Bit Error Rate
CDMA	Code Division Multiple Access
CFO	Carrier Frequency Offset
CN	Core Network
DECT	Digital European Cordless Telephone
DS-CDMA	Direct Sequence Code Division Multiple Access
EDGE	Enhanced Data rates for GSM Evolution
EPC	Evolved Packet Core
EPS	Evolved Packet System
ETACS	Extended Total Access Communication System
EUTRA	Evolved Universal Terrestrial Radio Access
FCC	Federal Communication commission
FDD	Frequency Division Duplex
FDMA	Frequency Division Multiple Access
FEC	Forward Error correction
FER	Frame Error Rate
FFT	Fast Fourier Transform
GSM	Global System for Mobile Communication
HARQ	Hybrid Automatic Repeat Request
HSDPA	High Speed Downlink Packet Access
HSPA	High Speed Packet Access

HSUPA	High Speed Uplink Packet Access
ICI	Inter Carrier Interference
IFFT	Inverse FFT
IMT	International Mobile Telecommunication
LTE	Long Term Evolution
MAC	Medium Access Control
MBMS	Multimedia Broadcast and Multicast Service
MCS	Modulation and coding scheme
NAS	Non-Access Stratum
OFDM	Orthogonal Frequency Division Multiplexing
OFDM	Orthogonal Frequency Division Multiplexing
OFDMA	Orthogonal Frequency Division Multiple Access
PAPR	Peak to Average Power Ratio
PBCH	Physical Broadcast channel
PCFICH	Physical Control Format Indicator Channel
PCS	Personal Communication Standard
PDCCH	Physical Downlink Control Channel
PDCP	Packet Data Convergence Protocol
PDN	Packet Data Network
PDSCH	Physical Downlink Share Channel
P-GW	Packet Data Network Gateway
PHICH	Physical Hybrid ARQ Indicator Channel
PMCH	Physical Multicast Channel
PMI	Precoding Matrix Indicator
POCSAG	POST Office Code Standard Advisory Group
P-SS	Primary Synchronization Signal
QoS	Quality of Service

RB	Resource Block
RLC	Radio Link Control
RRC	Radio Resource Control
RS	Reference Signal
RV	Redundancy Version
SAE	System Architecture Evolution
SC_FDMA	Singe Carrier Frequency Division Multiple Access
SC-FDMA	Single Carrier Frequency Division Multiple Access
SCTP/IP	Stream Control Transmission Protocol/ IP
S-SS	Secondary Synchronization Signal
TDD	Time Division Duplex
TDMA	Time Division Multiple Access
TDMA	Time Division Multiple access
UE	User Equipment

Chapter 1. **Introduction to Wireless Communication**

1.1 History of Wireless Communication

In the 1700s, people used primitive methods for transferring information and messages from one place to another, but these methods varied according to the distance and length of the message. For example, short messages, smoke signs, special flags, or other visual signals were used for short distance communication. However, to send a long message over a far distance, using couriers was a more viable elementary option.

The first visual telegraph systems, called semaphores, were built in 1792 and 1974 in France and Sweden, respectively, and were based on pulleys rotating wood beams or shutters. There were attempts to employ electrical telegraphy in 1809 by using separate wires to present letters and numbers in order to send messages over some kilometers of distance. In 1839, the electromagnetic telegraph was improved in England by applying deflections of needles to represent messages.

Figure 1.1 The first telegraph by Samuel Morse

In 1838, the Samuel Morse and Alfred Vail proposed a version of the electrical telegraph that included a logging device to record the message on paper tape (shown in Figure 1.1). This turning point in the development of the telegraph led to construction of more than 32,000 kilometers of telegraph lines in the United States by 1851.

Alexander Graham Bell invented the conventional telephone system in 1876 and contributed to the development of inter-city telephone lines in the United States by the end of the 1880s. The world's first wireless telephone call between Bell and Charles Taiter took place in 1880 via modulated light beam.

Gugliemo Marconi demonstrated the capabilities of radio transmission by transmission of Morse code via electromagnetic waves over 3 kilometers of distance. This invention caused an immense development in telecommunications.

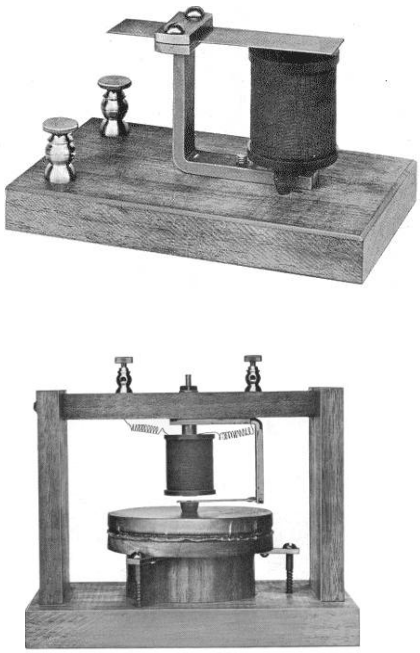

Figure 1.2 First telephone Device by Bell

This application highly used in military and during the Anglo-Boer war in 1899. In the early 1900s, the modern radio was invented and the first commercial radio station was established by 1920 in Pittsburgh (Detroit Station).

By 1934, municipal police radio systems were using AM (Amplitude Modulation) mobile communication systems in the U.S. FM (Frequency Modulation) was introduced by Edwin Armstrong and was widely used in mobile communication systems until the late 1930s. World War II increased the application and capabilities of wireless communications.

1.2 Mobile Radio Systems in the United States

The first public mobile telephone service used in 25 cities in the United States in 1946 had a single high power transmitter and large tower. In the late 1940s, push-to-talk telephone systems used 120 kHz of RF bandwidth in a half duplex mode. In reality, telephone-grade speech used only 3 kHz and the rest of the spectrum comprised RF filters and amplifiers. Later, the voice spectrum increased and the bandwidth decreased to 30 kHz.

In the 1950s and 1960s, Improved Mobile Telephone Service (IMTS) was developed. As a result, telephone companies provided services such as auto dial, full duplex, and auto trunking. Furthermore, telecommunications companies such as Bell Laboratories and AT&T provided a new concept of dividing coverage area in small cells. Each of these cells reuses portions of the spectrum in order to increase spectrum usage at the expense of greater system infrastructure [1]. In 1986, AT&T came up with the idea of cellular mobile systems, but these systems could not be implemented until the 1970s. The Advanced Mobile Phone System (AMPS) can be considered as the first U.S. cellular telephone system that was established by Ameritech in Chicago. In 1983, the Federal Communications Commission (FCC) allotted 666 duplex channels to the U.S. Advanced Mobile Phone System and in 1989 added 169 additional channels to U.S. cellular services.

Figure 1.3 Mobile Evolution

The first U.S. digital cellular (USDC) system hardware was installed in major U.S. cities in 1991. Electronic Industry Association Interim Standard IS-54 is the USDC standard that provides substitution of analog single-user channels to digital channels that can support three users in the same 30 kHz bandwidth. USDC capacity improved to triple AMPS capacity resulting from digital modulation used in USDC. Moreover, USDC took advantage of Time Division Multiple Access (TDMA) instead of Frequency Division Multiple Access (FDMA), and used channel coding technology to increase the capacity to six users for 30 kHz of bandwidth.

Code Division Multiple Access (CDMA)-based systems were introduced by Qualcomm Inc. and standardized by the Telecommunications Industry Association (TIA) as an Interim Standard (IS-95) in 1993. CDMA systems provide a large improvement in capacity mainly because of smaller signal-to-noise ratio than in systems using narrowband FM techniques. The development of wireless communication continued up

to and through the 1990s. New standards were introduced by different companies and organizations to achieve better performance. Table 1.1 shows different mobile radio standards in use in North America until 1994.

Table 1.1 Major Mobile Radio Standards in North America [1]

Standard	Type	Year of Introduction	Multiple Access	Frequency Band	Modulation	Channel Bandwidth
AMPS	Cellular	1983	FDMA	824-894 MHz	FM	30 kHz
NAMPS	Cellular	1992	FDMA	824-894MHz	FM	10 kHz
USDC	Cellular	1991	TDMA	824-894MHz	π/4-DQPSK	30 kHz
CDPD	Cellular	1993	FH/Packet	824-894MHz	GMSK	30 kHz
IS-95	Cellular/ PCS	1993	CDMA	824-894MHz 1.8-2 GHz	QPSK/ BPSK	1.25 MHz
GSC	Paging	1970s	Simplex	Several	FSK	1.25 kHz
POCSAG	Paging	1970s	Simplex	Several	FSK	1.25 kHz
FLEX	Paging	1993	Simplex	Several	4-FSK	15 kHz
DCS-1900(GSM)	PCS	1994	TDMA	1.85-1.99 GHz	GMSK	200 kHz
PACS	Cordless/ PCS	1994	TDMA/ FDMA	1.85-1.99 GHz	π/4-DQPSK	300 kHz
MIRS	SMR/PCS	1994	TDMA	Several	16-QAM	25 kHz

Table 1.2 Major Mobile Radio Standards in Europe [1]

Standard	Type	Year of Introduction	Multiple Access	Frequency Band	Modulation	Channel Bandwidth
E-TACS	Cellular	1985	FDMA	900 MHz	FM	25 kHz
NMT-450	Cellular	1981	FDMA	450-470 MHz	FM	25 kHz
NMT-900	Cellular	1986	FDMA	890-960 MHz	FM	12.5 kHz
GSM	Cellular/ PCS	1990	TDMA	890-960 MHz	GMSK	200 kHz
C-450	Cellular	1985	FDMA	450-465 MHz	FM	20 kHz/ 10kHz
ERMES	Paging	1993	FDMA	Several	4-FSK	25 kHz
CT2	Cordless	1989	FDMA	864-868 MHz	GFSK	100 kHz
DECT	Cordless	1993	TDMA	1880-1900 MHz	GFSK	1.728 MHz
DCS-1800	Cordless/ PCS	1993	TDMA	1710-1880 MHz	GMSK	200 kHz

1.3 Mobile Radio Systems around the World

At the same time mobile standards were being introduced in the United States, wireless standard developers were introducing their standards in Europe and Japan, as shown in Table 1.2 and 1.3 respectively.

The first cellular system in Japan was introduced in 1979 by Nippon Telephone and Telegraph Company (NTT). It was designed for 600 FM duplex channels in 800 MHz bandwidth. The most common cordless telephone standards in Europe and Asia are CT2 and Digital European Cordless Telephone (DECT). Microcell is used in CT2 for distances less than 100 meters. CT2 also uses Frequency Shift Keying (FSK) with a special speech decoder called adoptive differential pulse code modulation (ADPCM) for high quality voice transmission.

Table 1.3 Major Mobile Radio Standards in Japan [1]

Standard	Type	Year of Introduction	Multiple Access	Frequency Band	Modulation	Channel Bandwidth
JTACS	Cellular	1988	FDMA	860-925 Mhz	FM	25 kHz
PDC	Cellular	1993	TDMA	810-1501 MHz	π/4-DQPSK	25 kHz
NTT	Cellular	1979	FDMA	400/800 MHz	FM	25 kHz
NTACS	Cellular	1993	FDMA	843-925 MHz	FM	12.5 kHz
NTT	Paging	1979	FDMA	280 MHz	FSK	10 kHz
NEC	Paging	1979	FDMA	Several	FSK	10 kHz
PHS	Cordless	1993	TDMA	1895-1907 MHz	π/4-DQPSK	300 kHz

The development of wireless communication standards is still going on today, and the competition between various standard developers is intense. Chapter 2 (Backgroung) provides more information on current developments and standards.

Chapter 2. **Background**

Wireless communication networks were significantly advanced by the introduction of the cell concept by Bell Lab which provided a practical enhancement of mobile telecommunications system capacity. This can be achieved by dividing the coverage area into a given number of cells and assigning a specific frequency to each cell [1].

As described in chapter 1 (Introduction to Wireless Communication), the first generations of mobile communication networks were analog cellular systems that used Frequency Modulation (FM) for radio transmission. AMPS and ETACS were the most popular first generation mobile communication systems employed around 1983. The 2nd

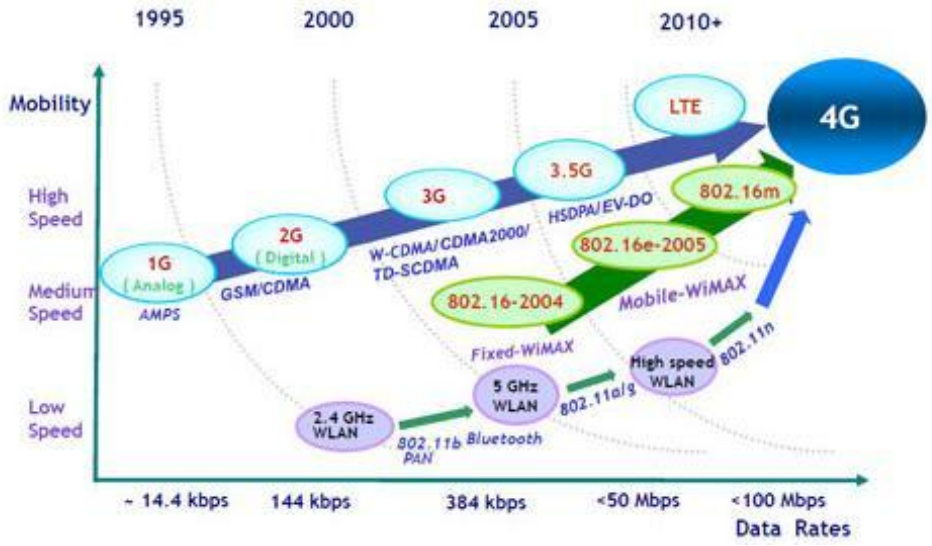

Figure 2.1 Wireless communication evolution track toward 4G.

generations of mobile communication standards were developed around 1995; these standards used digital modulation and provided three times more spectrum efficiency compared to the first generation. GSM and CDMA 2000 are two well known 2nd generation standards that were introduced by 3GPP and 3GPP2 standard development groups. GSM is based on Time Division Multiple Access (TDMA) while CDMA 2000 uses Code Division Multiple Access (CDMA). The 2nd generation was the beginning of the evolution toward 3G and 4G standards. 3GPP, IEEE and 3GPP2 are three major standard development groups that are in tight competition to satisfy 4th generation requirements.

LTE, also called EUTRA, introduced by 3GPP is a 3rd generation of mobile communication standard that uses Orthogonal Frequency Division Multiplexing (OFDM) in downlink and Single Carrier-Frequency Division Multiple Access (SC-FDMA) in uplink, whereas previous 3rd generation standards were using CDMA. Another adaptation of LTE is in packet-switched networks, which do not follow the circuit switching of preceding standards. The most frequent rival of LTE is the 802.16e standard, also called WiMAX that was developed by IEEE. Figure 2.1 shows the evolution track of 3G toward 4G. The main objectives of this evolution track are improvements in data rate, spectral efficiency, power consumption of the terminal, cell edge bit rate; and reductions in transmission latency, connection establishment latency and cost [2].

The first release of 3G provided by 3GPP in 2000 was called ‘Release 99’ for defining W-CDMA and UMTS standards. This evolution was followed by Release 4 in 2001, which added a given feature to Release 99 called ‘all-IP core network’. Release 5

introduced High Speed Downlink Packet Access (HSDPA) in 2002 followed by Release 6 that introduces High Speed Uplink Packet Access (HSUPA) and adds more features to the preceding release such as MBMS and integrated operation with Wireless LAN in 2005. Release 7 (from 2005 to 2007) introduced HDPA+, which focuses on developing specifications like latency and QoS improvement, and real time applications. Release 8 is the first LTE release and was published in 2008. Release 9 includes SAES enhancement, WiMAX and LTE interoperability. Release 10 is under development to satisfy International Mobile Telecommunications (IMT)-advanced requirements for 4th generation broadband mobile communications.

IMT-Advanced, previously known as "system beyond IMT-2000" is a concept introduced by the International Telecommunications Union (ITU). The main objective of IMT-Advanced is to develop a wireless communication technology that supports high data rates with high mobility and can be deployed in some areas by 2015. The requirements of IMT-Advanced are a peak data rate of 100 Mbps in high mobility (300 km/h) and 1 Gbps in low mobility (3 km/h). Table 2.1 outlines the peak data rates for 3GPP standards.

Table 2.1 Peak data rates and latency for 3GPP standards

3GPP Standards	Downlink Peak Data Rate	Uplink Peak Data Rate	Latency Round Trip Time
WCDMA (UMTS)	384 kbps	128 kbps	150 ms
HSDPA/ HSUPA	14 Mbps	5.7 Mbps	100 ms
HSPA +	28 Mbps	11 Mbps	50 ms
LTE	300 Mbps	75 Mbps	10 ms
LTE-Advanced	1 Gbps	500 Mbps	Less than 5ms

Chapter 3. **Problem Statement**

The physical layer performance of LTE is outlined in literature. Different values are stated as LTE performance that depend on parameters such as system bandwidth, multi antenna schemes, FDD or TDD operation, etc. The maximum data rate of LTE varies from 100 Mbps to 300 Mbps. There is no sufficient clue of how this value is calculated.

The main objective of this study is to determine physical layer throughput of LTE Release 8 in different scenarios for uplink and downlink. TDD and FDD operations are considered as separate scenarios in this study. Based on the system bandwidth that varies from 1.4 to 20 MHz, different amount of physical resources (from 10080 to 168000) are available during a radio frame. Physical channels and reference signals are mapped to these resources. By calculating the overhead of reference signals that actually do not carry information to higher layers and control channels that convey control information, we can determine the number of resource elements allotted for data transmission. Based on different modulation schemes, code rates, and number of antenna ports, the throughput for data channels can be calculated.

In TDD operation there are seven configurations for time domain multiplexing of downlink and uplink data transmission that lead to different throughput values in a given channel bandwidth.

Chapter 6 (proposed problem study) provides the number of resource elements available for data channels in different conditions. Chapter 7 (modeling and simulation) describes the physical layer procedure for data transmission in uplink and downlink, and Chapter 8 (Results and analysis) provides the link level simulation results and realted discussions.

Chapter 4. **Literature Review**

Different characteristics and features of LTE have been presented in the literature. Most of the research on LTE started in 2007 since the first release of this standard by 3GPP. This chapter provides a brief review on publications in different conferences and journals. Since the main objective of this study is the comprehensive analysis of LTE performance, the literature review is related but not limited to materials regarding performance, features and techniques of the physical layer. This chapter consists of three major sections. Section 1 gives an overview of published materials on LTE specifications and technologies. Section 2 outlines studies that analyze the performance of LTE. Section 3 discusses publications about comparison between LTE and other communication standards. Studies regarding other topics of LTE that are not mentioned in preceding sections are included in Section 4.

4.1 LTE Specifications and Features

A comprehensive description of the link layer protocols and the interaction between protocol layers is discussed in [8]. Compared with other UTRAN protocols, LTE provides less delay and overhead. Moreover, the interaction between protocol layers is more efficient. For example, the MAC and RLC layers are interact with each other with two layer ARQ functionalities, and scheduling in MAC and segmentation in RLC are interworking properly. As a result of appropriate layer interactions, the LTE protocol

header has low overhead. Furthermore, UE advanced sleep mode and handover techniques are described and outlined.

In [7], the authors give an overview of LTE characteristics and study different features such as physical layer specifications, multi antenna transmission, and intra-cell interference coordination. Moreover, LTE spectral efficiency for uplink and downlink is evaluated under specific conditions.

High level protocol operations and functions are discussed in [16]. This document explains elementary concepts of LTE protocols such as scheduling, quality of service, handovers and power save operations. In [17] a comprehensive overview of physical layer basics and parameters is provided. Resource block configuration, physical channels and modulation schemes are discussed.

4.2 LTE Performance analysis

In [9], some of the features of LTE are discussed such as MIMO, channel coding, and scheduling. Performance analysis in this paper is limited to downlink SISO and 2x2 MIMO scenarios. This paper mainly focuses on outlining the impact of different features of LTE on performance. However, at the time of this publication, some characteristics of LTE were under development, e.g., channel coding and rate matching, 4x4 MIMO. For example Figure 4.1 shows the impact of 2 antenna ports on spectral efficiency or Figure 4.2 illustrates the coding gain for 16-QAM and 64-QAM modulations by using turbo coding.

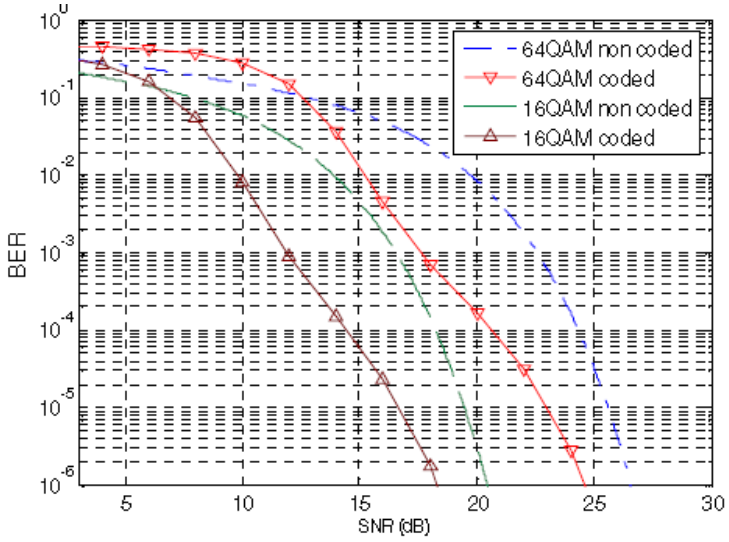

Figure 4.2 BER results with and without coding for 16 QAM and 64 QAM [9]

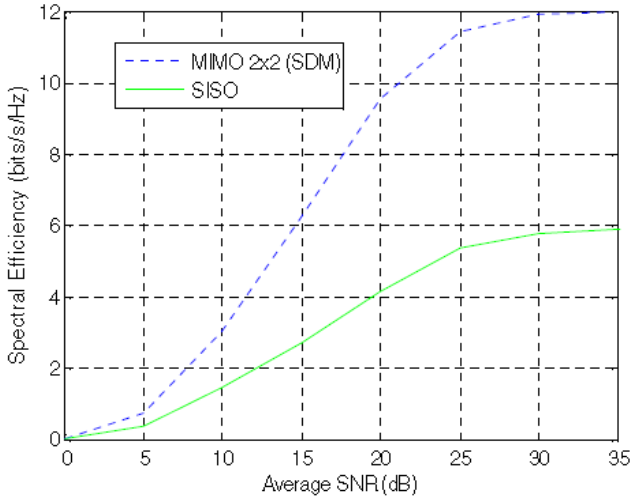

Figure 4.1 Spectral Efficiency for SISO and MIMO 2x2 with spatial division multiplexing scheme [9]

In [14] the performance of single user MIMO (SU-MIMO) is studied with two multi stream MIMO schemes including Per Antenna Rate Control (PARC) and Pre-Coded MIMO (PREC) in two different simulation environment.

Simulation Cases	CF (GHz)	ISD (meters)	BW (MHz)	PLoss (dB)
1	2.0	500	10	20
3	2.0	1732	10	20

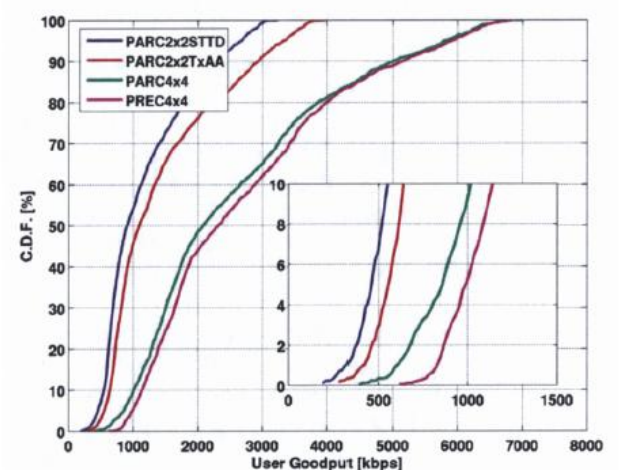

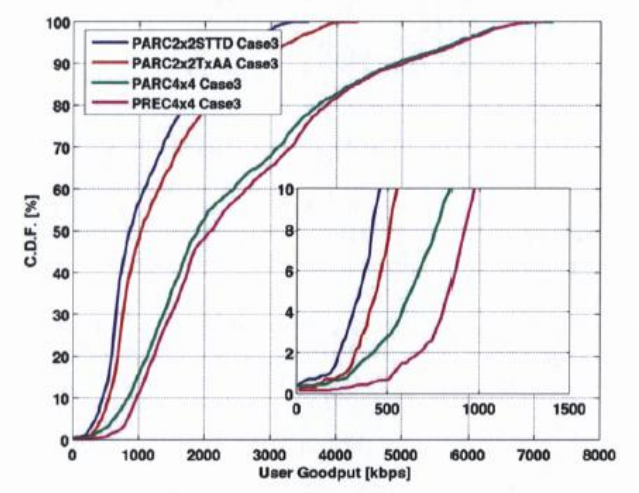

Figure 4.3 User Throughput CDF for Case1 and case3 of simulation environment [14]

Both schemes can have four transmit and four receive antenna. It is concluded that the average sector throughput performance of the four stream scheme is 75-90% higher than the one with two stream schemes. Also, based on the comparison of two different four-stream schemes (PARC4x4 and PREC 4x4), PERC schemes seem to be better in average sector throughput gain (5-6%) and coverage gain (13-20%). Figure 4.3 shows the simulation results for case 1 and case 3.

Performance study in [20] is limited to downlink transmission by using a MAC layer simulator. The main focus of this study is on evaluating the channel estimation method performance in Wiener low complexity (Wlc). Different estimation error impacts are investigated such as SNR estimation error, Doppler frequency estimation error, and PDP estimation error.

Simulation results are based on 10 MHz system bandwidth, one transmit and two receive antenna (SIMO). LTE downlink performance is evaluated based on the EVA channel and Wlc channel estimation method; however, high code rate and multi antenna schemes are not considered in performance analysis. Figure 4.4 shows the performance simulation results in this paper. This simulation is based on EVA channel and shows 5Mbps, 13 Mbps, and 31 Mbps of throughput for QPSK 1/3, 16 QAM ½ and 64QAM ¾ respectively. it is assumed that one antenna port is used.

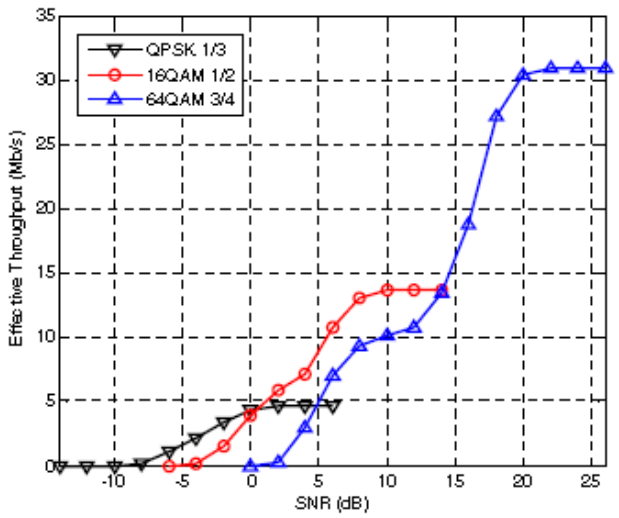

Figure 4.4 LTE throughput for a EVA channel with Doppler frequency 5Hz [20]

The main technical features of LTE are presented in [21], including MIMO, turbo coding used in LTE, and HARQ techniques. This paper also presents a performance analysis for 10 MHz of channel bandwidth, MIMO 4x4 and 2x2 in downlink and MIMO 1x2 in uplink cases. Figure 4.6 shows the spectral efficiency of LTE for uplink and downlink. The downlink control channel overhead is assumed to be 2 OFDM symbols per subframe, and a 0.93 code rate is considered. Based on these assumptions, the maximum throughput of the downlink and uplink is stated to be around 130 Mbps and 40 Mbps, respectively (Figures 4.5 and 4.7) . This paper also includes an overview of the next LTE release (LTE-Advanced, release 10) which is under development.

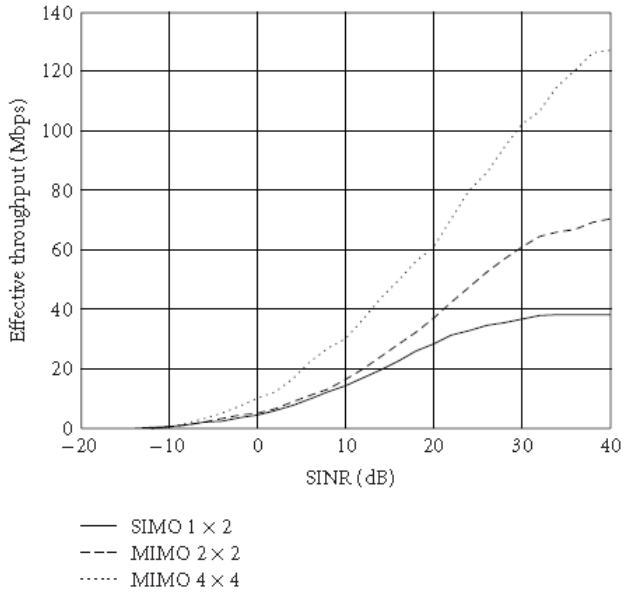

Figure 4.5 Link level simulation of throughput versus SINR in LTE downlink [21]

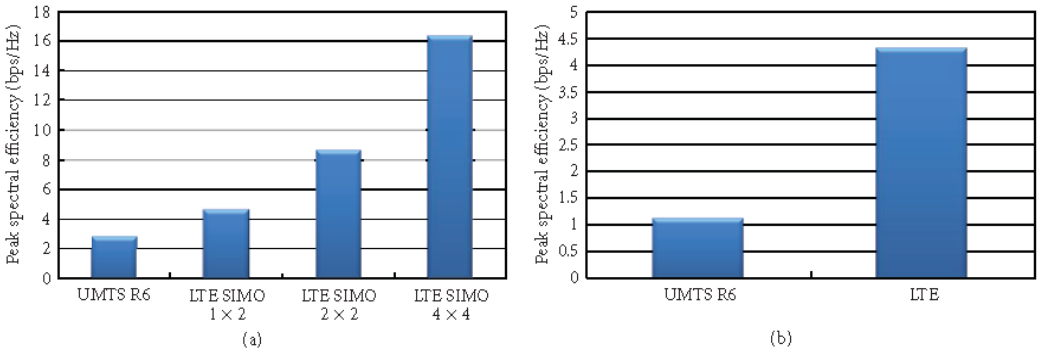

Figure 4.6 LTE peak spectral efficiencies in downlink (a) and uplink (b) [21]

In addition to conference and journal publications, 3GPP itself provides the maximum throughput of downlink and uplink as two report documents, [22] and [23] respectively.

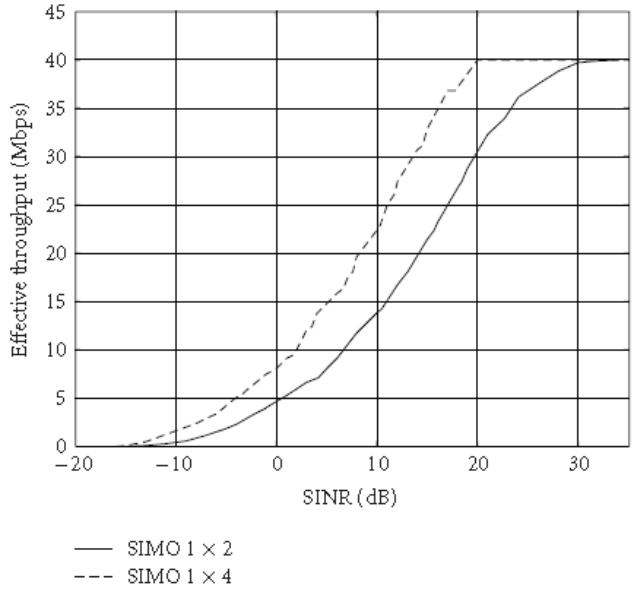

Figure 4.7 Link level evaluation of throughput versus SINR in LTE uplink [21]

Reference [22] states the maximum throughput of downlink as 326.4 Mbps in the case of four antenna ports, one OFDM symbol assigned for PDCCH, 20 MHz system bandwidth, 64-QAM modulation scheme and code rate of 1. Besides the code rate that is assumed to be 1, this calculation excludes reference signals and PDCCH. Also, [23] indicates that the maximum uplink throughput is 86.4 for 20 MHz system bandwidth, one transmit antenna, and 64-QAM modulation.

4.3 LTE characteristics and performance compared to other wireless communication standards

LTE is compared to WiMAX in [11] with respect to spectrum efficiency, average user throughput, and cell edge bit rate gains for both TDD and FDD operations. Based on

spectrum efficiency and average user throughput comparison, LTE outperforms WiMAX by about 60%. However, in uplink LTE is 100% better in cell edge and average performance. Figure [11] shows the spectral efficiency versus C.D.F for uplink and downlink.

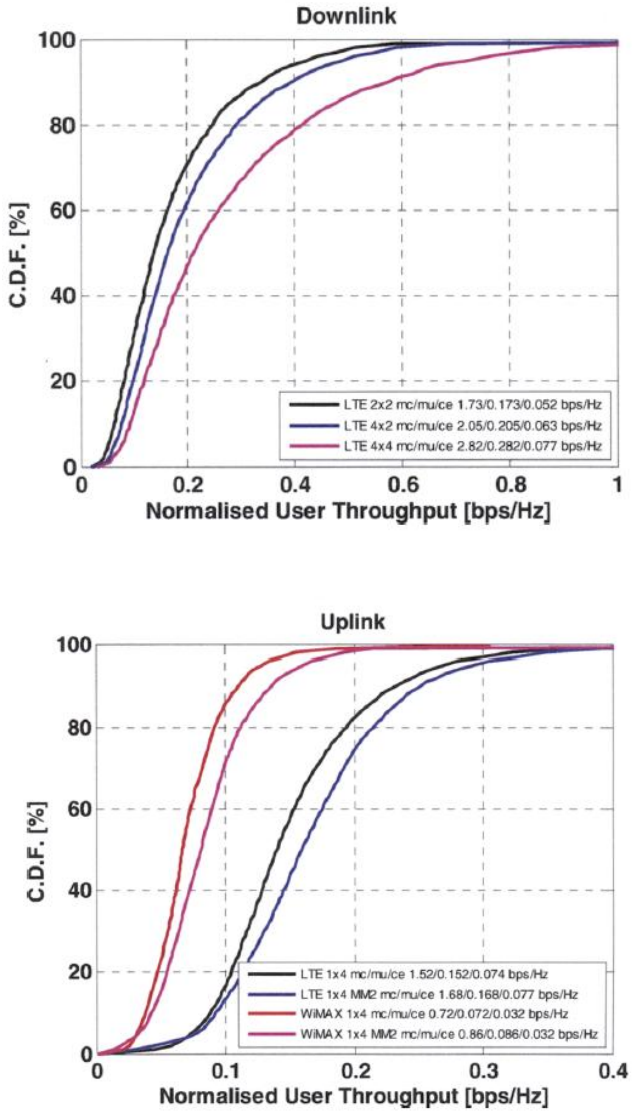

Figure 4.8 Summary of downlink and results with additional antenna concepts [11]

Performance comparison of LTE and WiMAX in [10] is based on Downlink FDD operation. This study compares the physical layer structure and gives the overhead for control channels for both standards. The results show better radio performance for LTE due to less overhead. The throughput calculation includes control and broadcast channel, however excludes the reference signal. Figure 4.9 shows the performance of two standards with 2 antenna ports. In terms of SNR gain both standards have the same performance, but in respect to the throughput, LTE outperforms WiMAX [10].

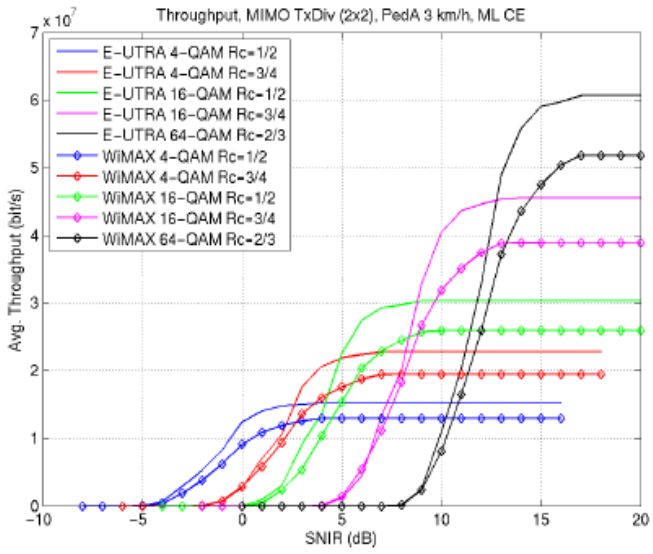

Figure 4.9 Average throughput in case of MIMO 2x2 Diversity for PedA 3 km/h (zero spatial correlation) and ML channel estimation algorithm for 20 MHz bandwidth (including all overhead)[10]

Beside radio access performance and spectrum efficiency comparison, similar specifications and technologies are collated in different documents. Figure 4.10 shows 2x2 MIMO throughput in case of vehicular A channel.

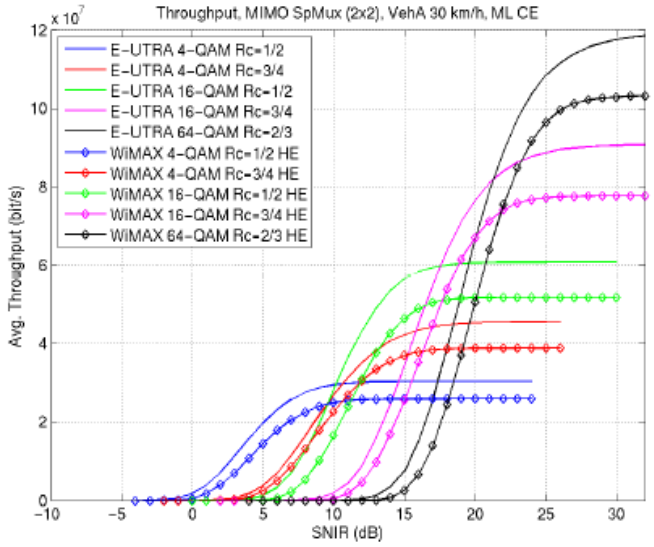

Figure 4.10 Average throughput for 20 MHz bandwidth in case of MIMO 2x2 Spatial Multiplexing for spatially uncorrelated vehicularA 30 km/h and ML channel estimation algorithm (incl. all overhead) [10]

For example, by virtue of the crucial role of MIMO schemes in performance of wireless communication networks, MIMO technologies are compared for WiMAX, LTE and LTE-advanced in [24]. In addition, [13] describes relay technologies for both communication standards and shows that by taking advantage of relay technologies, service coverage and system throughput is improved effectively.

4.4 Other LTE Topics

Considering the 3GPP evolution track, LTE-Advanced standardization is under development and the specifications and new technologies used in this version of 3GPP standards are discussed in some literature. In [25] a brief overview of Release 8 is provided, followed by LTE-Advanced requirements and technologies such as carrier

aggregation, evolved MIMO schemes for uplink and downlink, etc. This article also provides peak spectral efficiency and radio access performance for uplink and downlink of LTE-Advanced. In [26] carrier aggregation, a critical technology used in LTE-Advanced that impacts the peak data rate and spectral efficiency is described in detail.

Different MU-MIMIO schemes in Release 8 are verified in [27] by system level simulation and comparison to the zero-forcing technique of LTE-Advanced.

Chapter 5. LTE Protocol Concepts and Details

5.1 LTE General Architecture

5.1.1 EPS Architecture

System Architecture Evolution (SAE) is the evolution associated with the core network along with the radio access technology, indicated as LTE. SAE was developed to satisfy the requirements of LTE and provide improved data capacity, reduced latency and cost (capital expenditure and operational expenditure), and support for packet switch configuration. Hence LTE architecture consists of two main parts: EUTRAN (EUTRA Node) and EPC (Evolved Packet Core). These two nodes together comprise an Evolved Packet System (EPS). EPS routes the IP packet with a given Quality of Service (QoS), called an EPS bearer, from the Packet Data Network Gateway (P-GW) to User Equipment (UE). Figure 5.1 illustrates the overall architecture of EPS [3].

5.1.2 Evolved Packet Node (EPC)

EPC includes the Packet Data Network Gateway (P-GW), Serving Gateway (S-GW), Mobility Management Entity (MME), Home Subscriber Service (HSS), Policy Control and Charging Rules Function (PCRF).

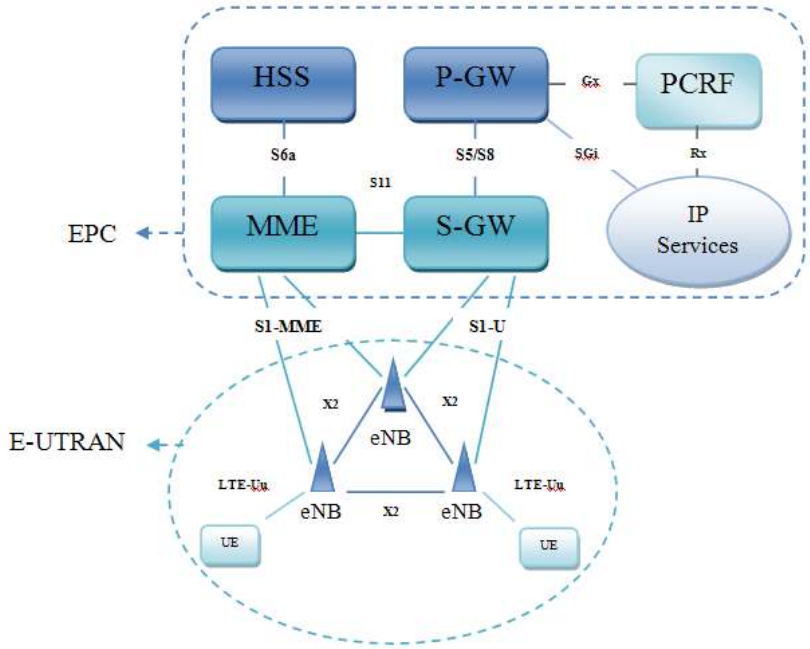

Figure 5.1 EPS Architecture [29]

P-GW can be considered as an IP anchor which connects UE to the external packet data network. P-GW also filters the downlink user IP packets and performs Policy enforcements. Moreover it can operate as a mobility anchor between 3GPP and non-3GPP technologies such as WiMAX or CDMA2000.

S-GW is a mobility anchor for the user plane when UE moves between eNodeBs. Further, user packets are transferred via S-GW; when UE is in its ideal state, bearer information is saved and maintained by S-GW. It also performs as mobility anchor between LTE and other 3GPP standards like UMTS and GPRS.

MME is responsible for user authentication by interacting with HSS, bearer management, ideal mode UE tracking, and choosing the SGW when Core Network (CN)

reallocation is needed. These functionalities are taking place by Non-Access Stratum (NAS) protocols that are running between UE and CN.

HSS contains the information on the Packet Data Networks (PDNs) to which the UE can connect, such as Access Point Name (APN) or a PDN address. It also includes the users' SAE subscription data and information on the MME with which the UE is interacting.

PCRF performs policy control and manages charging functionalities in the Policy Control Enforcement Function of P-GW and authorizes QoS.

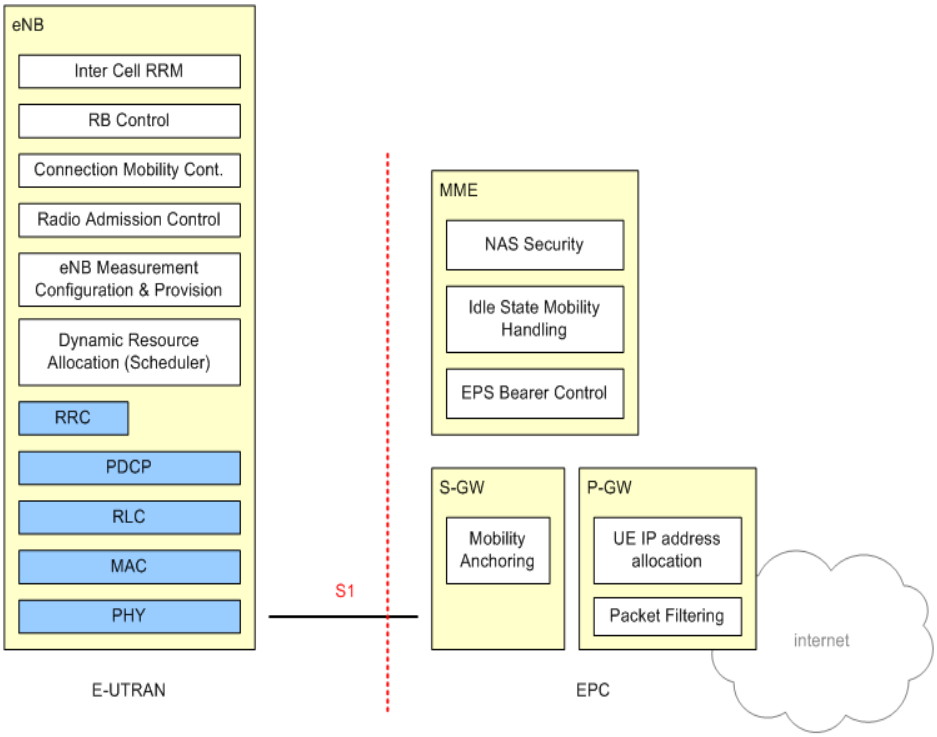

Figure 5.2 Functional split between E-UTRAN and EPC [3]

5.1.3 **Access Network (E-UTRAN)**

E-UTRAN essentially includes one node: the evolved Node B (eNodeB). eNB is actually the base station that is connected to UE which provides network air interface. One of the responsibilities of eNB is radio resource management relating to radio bearer control, radio admission, mobility control, and assignment of resources to UEs. In order to most efficiently use the radio interface, eNB is responsible for compressing the IP packet header to reduce the overhead. Security and encryption of data sent over the radio interface is another task performed by eNB. E-UTRAN architecture is said to be flat since there is no centralized controller in E-UTRAN [28].

EPS and E-UTRAN network components are connected to each other via standard interfaces. Figure 5.2 shows the functional split between E-UTRAN and EPC [3].

As shown in Figure 5.3-B, the user plane consists of PDCP (Packet Data Coverage Protocol), RLC (Radio Link Control), and MAC (Medium Access Control) sublayers that are terminated in eNB [3]. The tasks associated with these layers will be discussed later. Part A of Figure 5.3 illustrates the control plane that is similar to a user plane, instead of the compression header function that does not exist in control plane. The Access Strum protocol refers to the protocol between layers below the Non-Access Protocol (NAS), which is another protocol of the control plane [3].

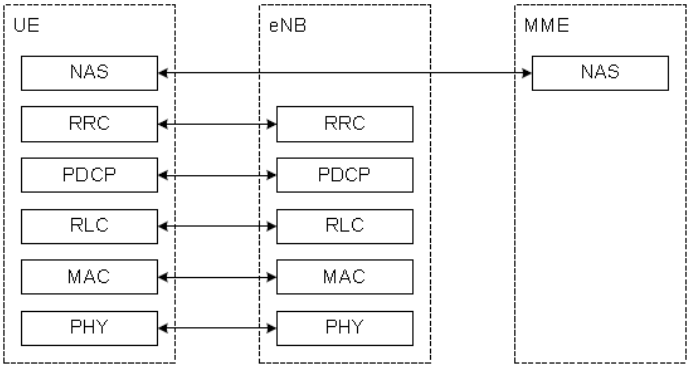

A. control plane

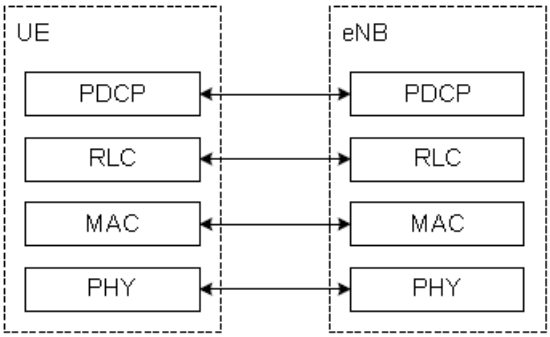

B. user plane

Figure 5.3 E-UTRAN user and control plane protocol stacks [3]

5.1.4 **E-UTRAN Network Interfaces**

The interface between EPC and eNB is an S1 interface. The S1 interface is indeed a protocol with mainly 5 layers. The S1-MME protocol stack (control plane protocol) includes a physical layer, data link layer, SCTP, and application layer; however, the five layers for S1-U (user plane protocol) are physical layer, data link layer, IPv6/IPv4, UDP and GTP-U. This interface is based on SCTP/IP (stream control transmission protocol/IP) that is reliable for message delivery. Furthermore, it controls multi-streams and avoids

multi-homing [28]. The inter-connection between eNBs is established by an X2 interface [39] that has the same user and control plane layers as S1[38].

5.1.5 LTE Protocol Layers

5.1.5.1 Radio Resource Control (RRC)

This protocol layer exists in the control plane only and is responsible for transferring dedicated and common NAS information. Dedicated NAS information is related to a specific UE; however, common NAS information is associated with all users. This layer also provides services such as establishment of paging, Signaling Radio Bearers (SRB), and handover. Besides establishment of the RRC connection, modification and release of this connection can be performed by this protocol layer. This layer can handle the information for UEs in RRC-IDLE, like notification of incoming calls, as well as information for RRC-CONNECTED, such as channel configuration information and handover information. RRC also provides Inter-RAT mobility and measurement configuration such as establishment, modification and release of intera-frequency, inter-frequency and inter-RAT mobility [31].

5.1.5.2 Packet Data Coverage Protocol (PDCP)

This protocol layer associates with both the control plane and user plane. In the control plane, RRC messages are processed by PDCP. In the user plane, PDCP deals with IP packet messages. Header recompression, and integrity protection and ciphering can be considered as main tasks performed by PDCP layer. Also, this layer provides retransmission and reordering procedures for handover [32].

5.1.5.3 **Radio Link Control (RLC)**

The main function of this layer is to organize the upper layer packets in a size capable of transmission over the radio interface. RLC also recovers packet losses by transferring radio bearers again to avoid transmission errors. This protocol also reorders packets that are received out of order due to the HARQ functionality that is performing in the layer below RLC [33].

5.1.5.4 **Medium Access Control**

The Medium Access Control (MAC) layer is responsible for multiplexing and de-multiplexing data between the physical layer and RLC. This layer consists of logical channels that are connected to physical channels for transmission data between the physical and Mac layers. The main functions of the Mac layer are: scheduling of radio resources between UEs, random access procedure, uplink timing alignment, discontinuous reception, and scheduling information transfer [34].

Figure 5.4 outlines the procedure data transmission from eNB to UE. Each layer receives a Service Data Unit (SDU) from a higher layer in the transmitter (e.g., MAC layer receives an SDU from RLC) and sends the Protocol Data Unit to the lower layer (RLC sends PDU to MAC layer).

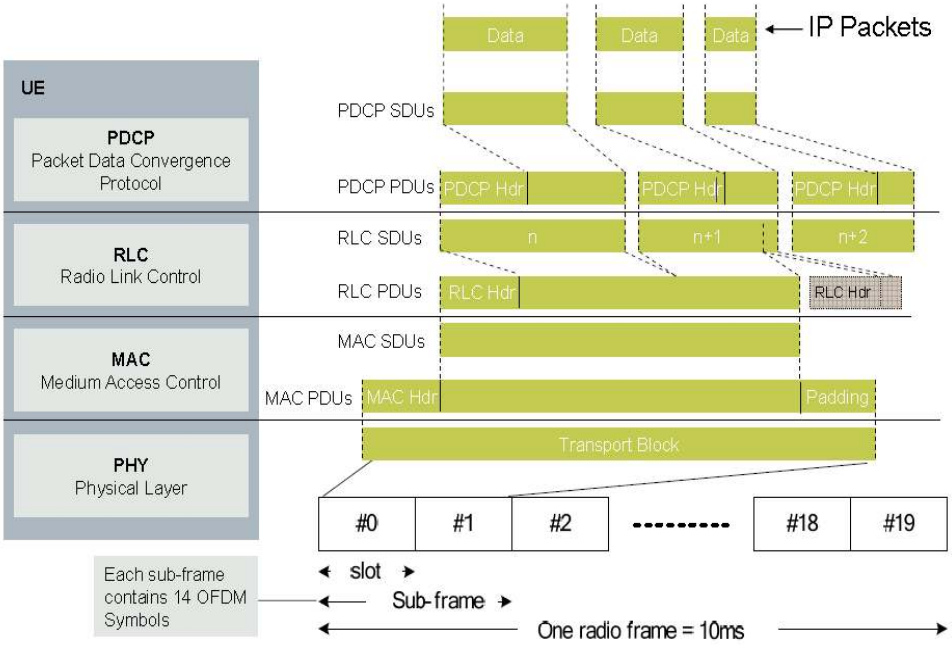

Figure 5.4 Downlink transmit procedure in time domain [16]

In this study, the main focus is the physical layer and its performance. This layer is related to the MAC layer as shown in Figure 5.5. Physical channels are mapped to transport channels to transfer data and control information from the physical layer to MAC layer. Transport channels on the higher level are connected to logical channels that relate the MAC layer to the RLC layer.

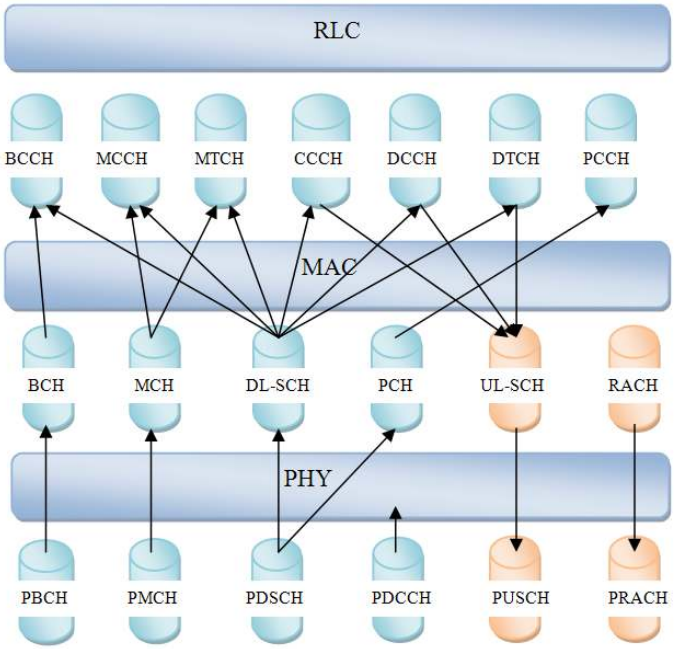

Figure 5.5 Downlink and uplink physical, transport and logical channel mapping

5.2 Physical Layer General Descriptions

5.2.1 Orthogonal Frequency Division Multiplexing (OFDM)

OFDM is used in LTE Downlink by virtue of simple implementation in receiver and high performance. In OFDM, Frequency selective wide band channel is divided into non-frequency selective narrowband sub-channels that are orthogonal to each other [28]. Each subcarrier is modulated based on conventional modulation schemes such as QPSK and 16-QAM.

Transmission of a high data rate stream results in an Inter Symbol Interference (ISI) problem. This problem arises from the fact that the channel delay spread is greater than the symbol period when data is transmitted as a serial stream. To avoid this problem in OFDM, the serial data stream is converted to M parallel subcarriers. This conversion guarantees that the symbol duration is now M times larger than the channel delay spread and avoids ISI. Figure 5.6 shows the block diagram of OFDM for receiver and transmitter.

As mentioned before, the serial-to-parallel block converts serial data to the M parallel subcarrier. Then subcarriers are individually modulated. Subcarriers can carry different data rates since the channel gain can be different between subcarriers due to the channel frequency selectivity [28]. The Inverse Fast Fourier Transform (IFFT) block converts M frequency domain data symbols to N complex time domain samples in a way $N \geq M$ [28]. One of the key steps in OFDM signal generation is to add Cyclic Prefix (CP) to avoid ISI. CP is generated by duplicating the last G samples of IFFT output symbol and adding them to the beginning of that symbol [28]. It should be considered that the length of G must be longer than the longest supported channel response. The final step is to convert the IFFT output symbols to serial data stream to be transferred through the frequency selective channel [28]. At the receiver the inverse process takes place to obtain ISI free symbols.

One of the remarkable disadvantages of OFDM is high Peak-to-Average Power Ratio (PAPR). Amplitude variation of OFDM symbols is high due to the fact that the time domain OFDM symbols can be considered as Gaussian waveform. Therefore, the OFDM

signal is distorted from nonlinear power amplifiers. To eliminate distortion, power amplifiers need to be operated with larger operating point that lead to expensive transmitters.

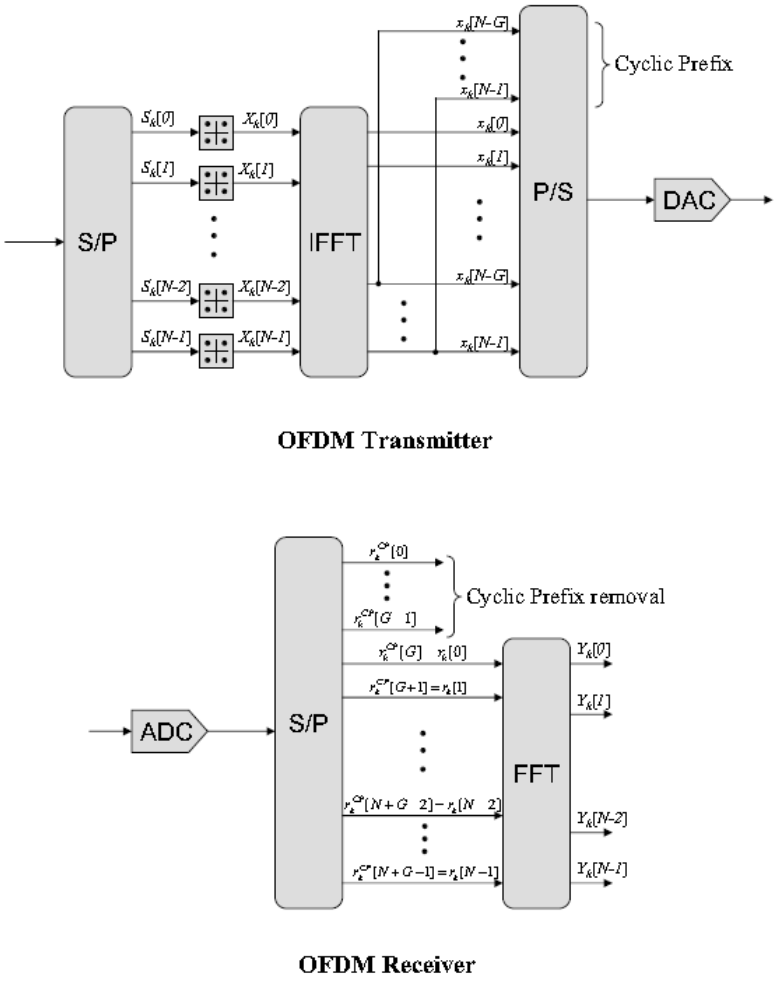

Figure 5.6 OFDM system Model [28]

Another significant problem of OFDM is that OFDM is sensitive to carrier frequency offset and time- varying channels. Different reference frequencies used in transmitter and receiver cause Inter-Carrier Interference (ICI) that contributes to lose OFDM orthogonality. Components that are used in the user terminal are cost effective, and the local crystal in the receiver may have more intense problems of drifting than the one in the transmitter. This can cause a Carrier Frequency Offset (CFO) that may be greater than subcarrier spacing. Even in cases where transmitter and receiver frequencies are synchronized, the impact of Doppler can cause frequency errors [28].

5.2.2 **Orthogonal Frequency Division Multiple Access (OFDMA)**

In OFDM All subcarriers at any given time are received by a single user; however, in OFDMA subcarriers are received by multiple users simultaneously, providing a multi-user scheme [28]. OFDMA can be used with the TDMA (Time Division Multiple Access) technique, meaning that a group of subcarriers is assigned to be transmitted during a specific time period [28].

5.2.3 **Single Carrier-Frequency Division Multiple Access (SC-FDMA)**

SC-FDMA is chosen over OFDMA and DS-CDMA (Direct Sequence Code Division Multiple Access) for uplink based on some significant benefits. DS-CDMA is used in UMTS. One of the disadvantages of this scheme is intra-cell interference, even in frequency selective channels, which leads to the reduction of channel capacity and inability to use adaptive modulation. Another disadvantage is the Pick to Average Power Ratio; that the OFDMA scheme also suffers from this problem. However, due to uplink-

downlink compatibility, OFDMA could be one of the considered schemes for LTE uplink.

SC-FDMA can satisfy all of the benefits mentioned for OFDM in addition to low PAPR. Similar to OFDM, the bandwidth is divided into multiple parallel subcarriers with cyclic prefix in between in order to stay orthogonal to each other and eliminate ISI.

In OFDM each subcarrier is modulated by data symbols individually in such a way that at a given time, each constellation point of digital modulation represents the amplitude of each subcarrier. However, in SC-FDMA, the linear combination of all data symbols that are transmitted at the same time is modulated to a given subcarrier. In a given symbol period, all transmitted subcarriers of a SC-FDMA signal are carrying a component of each modulated data symbol. This is known as a single carrier scheme of SC-FDMA.

SC-FDMA can be implemented both in a time domain and frequency domain. In LTE, frequency domain implementation is used since it is more bandwidth efficient compared to the time domain scheme. Figure 5.7 shows a frequency domain SC-FDMA.

Compared to Figure 5.6, we can consider some differences between these two schemes. After constellation mapping, each block of QAM data symbol is going through M- point DFT (Discrete Fourier Transform) operations. To reach the size of the N IFFT subcarrier, the output of DFT is zero padded. There are two schemes of subcarrier mapping: localized and distributed.

In a localized approach, M neighbor subcarriers are grouped together and this group is assigned to a single user that causes M-QAM data symbols at IFFT block output to convert to an interpolated version of the original ones. This is similar to a narrowband single carrier with a cp (equivalent to the time domain generation with repetition factor L=1) and 'sinc' (sinx/x) pulse shaping filtering (circular filtering).

Subcarrier distributed mapping groups M subcarriers within equal spaces, e.g., every L^{th} subcarrier, and inserts L-1 zeros between M DFT outputs before IFFT operations. Beside this approach of zero interpolation, zero padding takes place on either side of DFT output.

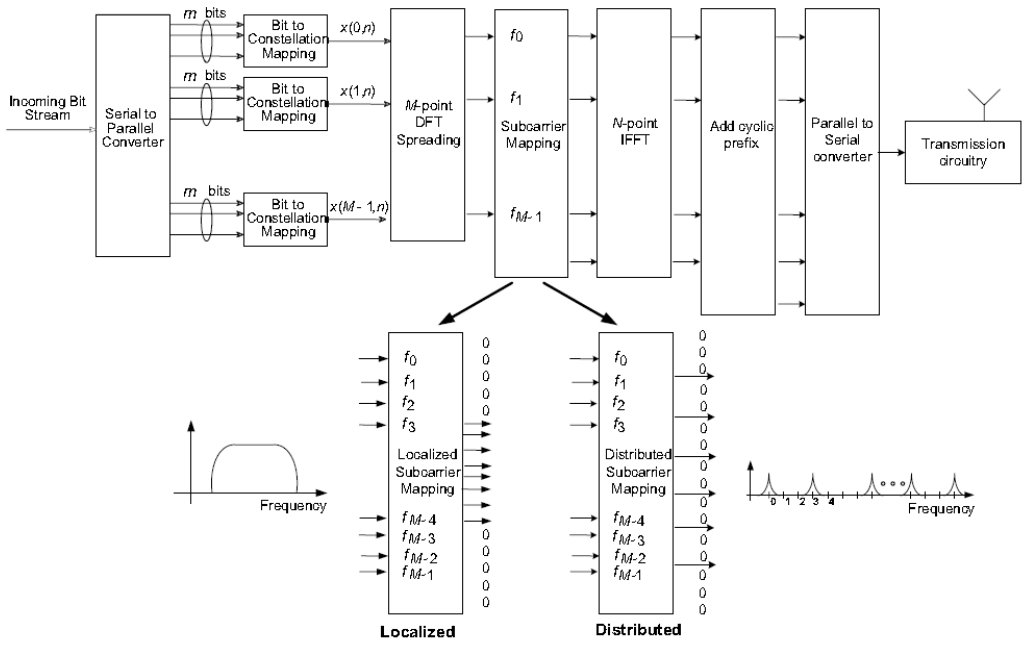

Figure 5.7 Frequency domain implementation of SC-FDMA [28]

Zeros inserted into both sides of the DFT output lead to unsampling, while zeros inserted between DFT outputs create waveform repetition in the time domain.

LTE employs localized subcarrier mapping, which best fits the requirements and configuration of this standard.

5.2.4 **Physical Layer – Basic Parameters**

Transmission parameters in LTE consist of frequency, space, and time to create transmission resources for carrying data. All of the time units in LTE are specified as a factor of $T_s = 1/ (15000*2048)$ in which 2048 is the FFT length. The LTE radio frame for downlink and uplink transmission is $307200* T_s = 10$ms long. LTE supports two radio frame structures: 1) FF, which uses type 1 frame structure, and 2) TDD, which is applicable to type2.

A radio frame consists of 10 subframes ($30720 * T_s = 1$ms long) in FDD and two half- frames ($153600* T_s = 5$ms long) in TDD. A half-frame is divided into four subframes and a special subframe, or five subframes, based on downlink to uplink switch point periodicity. A special subframe does not exist in second half frames with 10ms downlink to uplink switch point periodicity. The TDD frame structure can be configured in seven different subframe formats; however subframes 0 and 5 and DwTS are reserved for downlink transmission. The subframe that appears after special subframe as well as UpPTS, is always assigned to uplink transmission. Each subframe in both FDD and TDD has two slots of $15360 * T_s = 0.5$ ms. Figure 5.8 shows the LTE frame structure.

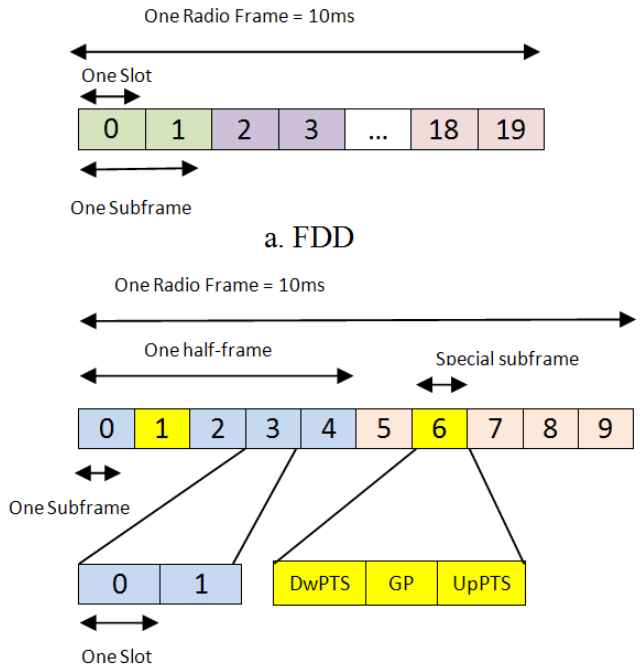

Figure 5.8 LTE frame structure [29]

In frequency domain 12, subcarriers are grouped together and make up the Resource Block (RB) in one slot. So a Resource Block occupies 180 KHz in the frequency domain and 0.5 ms in the time domain as shown in Figure 5.8. Based on the system bandwidth there are 6 to 110 RBs available for data transmission. Table 5.1 shows the resource block configuration for different channel bandwidths.

Table 5.1 Resource block configuration for different channel bandwidths [6]

Channel Bandwidth (MHz)	**1.4**	**3**	**5**	**10**	**15**	**20**
Number of RBs	6	15	25	50	75	100

Figure 5.9 illustrates the configuration of RBs in the time domain and frequency domain. The number of subcarriers and OFDM or SC-FDMA symbols in a resource block depends on the subcarrier spacing and cyclic prefix mode. Table 5.2 presents resource block parameters for both uplink and downlink transmission.

Table 5.2 Resource Block Parameters

		Normal Cyclic Prefix	Extended Cyclic Prefix	
		Subcarrier Spacing: 15kHz	Subcarrier Spacing: 15kHz	Subcarrier Spacing: 7.5kHz
Downlink	Number of OFDM Symbols	7	6	3
	Number of Subcarriers	12	12	24
Uplink	Number of SC-FDMA Symbols	7	6	-
	Number of Subcarriers	12	12	-

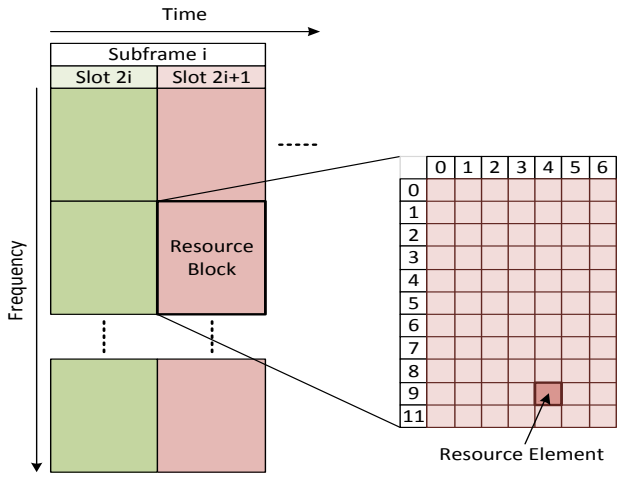

Figure 5.9 Resource Block Structure [29]

The TDD operation provides seven different configurations for subframes as shown in Table 5.3. Based on this table, in mode 5 the most possible subframes are assigned to downlink transmission; however mode 0 carries the most data for uplink transmission. In

TDD operation for switching between downlink to uplink transmission there is a guard period in the special subframe that allows advanced timing for uplink. The structure of the special subframe is outlined in Table 5.4.

Table 5.3 TDD frame configuration [6]

Uplink-Downlink configuration	Downlink-Uplink switch point Periodicity (ms)	Subframe number									
		0	1	2	3	4	5	6	7	8	9
0	5	D	S	U	U	U	D	S	U	U	U
1	5	D	S	U	U	D	D	S	U	U	D
2	5	D	S	U	D	D	D	S	U	D	D
3	**10**	D	S	U	U	U	D	D	D	D	D
4	**10**	D	S	U	U	D	D	D	D	D	D
5	**10**	D	S	U	D	D	D	D	D	D	D
6	5	D	S	U	U	U	D	S	U	U	D

Table 5.4 Special frame structure [6]

Special subframe configuration	Normal cyclic prefix in Downlink			Extended cyclic prefix in Uplink		
	DwPTS OFDM symbols	UpPTS SC-FDMA symbols		DwPTS OFDM symbols	UpPTS SC-FDMA symbols	
		Normal CP	Extended CP		Normal CP	Extended CP
0	3	1	1	3	1	1
1	9			9		
2	10			10		
3	11			11		
4	12			3	2	2
5	3	2	2	9		
6	9			10		
7	10			-	-	-
8	11			-	-	-

5.3 Physical Channels and Reference Signals

5.3.1 Downlink Structure and Specifications

Downlink transmission is carried out with assistance of the physical channels listed below:

PBCH: Physical Broadcast Channel

PDCCH: Physical Downlink Control Channel

PDSCH: Physical Downlink Share Channel

PCFICH: Physical Control Format Indicator Channel

PHICH: Physical Hybrid ARQ Indicator Channel

PMCH: Physical Multicast Channel

Beside the physical channels, there are reference signals that do not carry information from the upper layers and are used for synchronization and channel estimation:

P-SS: Primary Synchronization Signal

S-SS: Secondary Synchronization Signal

RS: Reference Signal

Before describing details of physical channels, we define some parameters used for mapping these channels to resource elements in downlink.

k: frequency domain index (subcarrier index)

l: time domain index (OFDM symbol index)

NRB_{dl} : number of resource blocks in downlink

NSB_{dl} : number of OFDM symbols for one resource block in downlink

NSC_{rb}: number of subcarriers in resource block

REG: Resource Element Group. A set of four physical Resource Elements

5.3.1.1 **PBCH**

Physical broadcast channel contains basic information for UE to access the cell. The number of bits transmitted by this channel is 1920 bits in the case of normal cyclic prefix and 1728 bits for extended cyclic prefix. PBCH information is transmitted within four radio frames in subframe 0 slot1. The resource elements indexes for PBCH transmission are specified with k and l as:

$$k = (NRB_{dl} * NSC_{rb}) /2 – 36 + k' \quad , k' = 0,1,\ldots,71$$

$$l = 0, 1\ldots 3$$

PBCH information is assigned to 72 subcarriers and 4 OFDM symbols. The information should be mapped to resource elements by increasing k and l indices, respectively. The resource elements that are used for reference signals cannot be used for PBCH information [6]. For instance, assuming that the system bandwidth is 1.4 MHz, in case of normal cyclic prefix and 15 kHz subcarrier spacing, $NRB_{dl} = 6$ and $NSC_{rb} = 12$, and $NSB_{dl} = 7$; therefore k = 0… 71 which fits to 6 resource blocks starting from subcarrier 0 in 1st resource block 0 to subcarrier 71 in 6th resource block in frequency domain and first to 4th OFDM symbols in the second slot of the first subframe. In case of 100 RBs, k = 564…635 which lies on the central 6 resource blocks (RB = 47 to 52). Generally PBCH is mapped to the 72 central subcarriers that allow UE to detect it before accessing the information about the system bandwidth [28].

There are two parts of broadcast system information: Master Information Block (MIB), used for cell access, and System Information Block (SIB) [28]. Downlink system bandwidth, PHICH structure, and the most significant 8 bits of the system frame number are included in MIB.

For reliable transmission, MIB is spread out over four consecutive radio frames so the probability of losing information due to channel fading decreases significantly [28]. Moreover, PBCH takes advantage of convolutional coding with 1/3 code rate. As a result, the code rate of MIB is very low and provides better error protection [28].

Table 5.5 Number of resource elements for PBCH in one radio frame

	4 antenna ports	2 antenna ports	1 antenna port
Number of REs assigned to PBCH for antenna port 0	240	264	276

Resource elements assigned for PBCH are shown in Table 5.5 for one, two and four antenna diversity. For different channel bandwidth that leads to different numbers of resource blocks, the number of resource elements allocated for PBCH is constant.

5.3.1.2 **PDCCH**

This channel conveys UE specific control information such as scheduling assignment, resource allocation of physical channels, and HARQ information. This channel is transferred by the first three OFDM symbols in each subframe. The number or resource elements assigned to this channel are varied based on the channel condition, transition scheme (MBSFN or Non-MBSFN modes described later) and number of resource blocks available for given bandwidth. Table 5.6 presents the number of OFDM symbols used for PDCCH.

Table 5.6 Number of OFDM symbols used for PDCCH [6]

Subframe	Number of OFDM symbols for PDCCH	
	NRB_{dl} >10	NRB_{dl} ≤10
Subframe 1 and 6 for TDD configuration	1,2	2
MBSFN subframes on a carrier supporting both PMCH and PDSCH for 1 or 2 cell specific antenna port	1,2	2
MBSFN subframes on a carrier supporting both PMCH and PDSCH for 4 cell specific antenna port	2	2
MBSFN subframes on a carrier not supporting PDSCH	0	0
All other cases	1,2,3	2,3,4

The modulation scheme for PDCCH is QPSK; modulated symbols are mapped to the resource elements of the first three OFDM symbols of each subframe that are not assigned for reference signals PHICH and PCFICH.

Table 5.7 summarizes total resource elements allocated for PDCCH in different scenarios.

Table 5.7 Number of resource elements assigned to PDCCH for antenna port 0 for one radio frame.

Number of OFDM symbol assigned for PDCCH	Number of antenna ports	NRB_{dl}					
		6	15	25	50	75	100
1	1	-	1500	2500	5000	7500	10000
	2	-	1200	2000	4000	6000	8000
	4	-	600	1000	2000	3000	4000
2	1	1320	3300	5500	11000	16500	22000
	2	1200	3000	5000	10000	15000	20000
	4	960	2400	4000	8000	12000	16000
3	1	2040	5100	8500	17000	25500	34000
	2	1920	4800	8000	16000	24000	32000
	4	1680	4200	7000	14000	21000	28000
4	1	2760	-	-	-	-	-
	2	2640	-	-	-	-	-
	4	2400	-	-	-	-	-

5.3.1.3 **PCFICH**

The number of OFDM symbols that used for PDCCH transmission in each subframe is specified by PCFICH. As seen in Table 5.6, there is no PDCCH for the subframes that are allocated to MBSFN therefore no PCFICH is needed. This channel carries 32 bits

using QPSK modulation. Therefore there are 16 symbols mapped to 16 resource elements in the first OFDM symbol of each subframe. The location of 16 resource elements associated with PCFICH is spread over frequency and divided into four resource element groups. Allocation of PCFICH resource element groups is based on a given pattern that depends on physical cell ID and is known by UE, so that UE can decode it easily.

5.3.1.4 **PHAICH**

When eNB receives a transmission on the PUSCH, it sends back ACK (0 for positive Acknowledgement) and NACK (1 for Negative Acknowledgement) through PHAICH. For robust transmission, three repetitions of ACK or NACK information are modulated to BPSK symbols. Each BPSK symbol is converted to a separate orthogonal Walsh sequence and each quadruplet is mapped to an OFDM symbol [28]. The number of OFDM symbols used for PHAICH transmission (1, 2 or 3 symbols that can be configured) is indicated by PBCH as well as the number of PHICH groups configured in the cell [28].

5.3.1.5 **PDSCH**

This physical channel is utilized for transmission of user data, broadcast system information that is not transmitted by PBCH, and paging messages [28]. PDSCH can map to any resource elements not used for other channels and reference signals. Modulation for this channel is QPSK, 16-QAM and 64 QAM. Table 5.8 outlines the resource elements used for PDSCH in different system bandwidths and antenna diversity.

Table 5.8 presents the number of resource elements for antenna port 0 for each scenario, meaning that in case of more than one antenna port, the total number of

resource elements available for PDSCH transmission is a factor of two or four of a given value. For instance, the total resource element for 100 RBs and four layers of diversity, assuming there is just one OFDM symbol allocated for PDCCH, is 541888 (135472*4).

PDSCH data are transmitted as a transport block to/from the MAC layer within a time transmit interval (TTI equals to 1 ms). A maximum of two transport blocks can be transmitted via a TTI, depending on the transmission mode [28].

Table 5.8 PDSCH resource elements for antenna port0 in one radio frame

Number of OFDM symbol assigned for PDCCH	Number of antenna ports	NRBdl					
		6	15	25	50	75	100
1	1	-	21936	36936	74436	111936	149436
	2	-	21048	35448	71448	107448	143448
	4	-	19872	33472	67472	101472	135472
2	1	7716	20136	33936	68436	102936	137436
	2	7368	19248	32448	65448	98448	131448
	4	7152	18672	31472	63472	95472	127472
3	1	6996	18336	30936	62436	93936	125436
	2	6648	17448	29448	59448	89448	119448
	4	6432	16872	28472	57472	86472	115472
4	1	6276	-	-	-	-	-
	2	5928	-	-	-	-	-
	4	5472	-	-	-	-	-

There are two schemes for allocating data to physical resource blocks known as Localized Mapping and Distributed Mapping. In localized mapping, two resource blocks in one subframe (pair of resource blocks) are assigned to the same UE. In distributed mapping, however, each resource block in a slot can be allotted for UE. Therefore in a distributed scheme, data are mapped to different frequencies for the same UE [28]. Figure 5.10 illustrates distributed mapping.

Distributed data mapping leads to frequency hopping, where so that a block of data is mapped to one set of 12 subcarriers and the other block of data is assigned to another set of 12 subcarriers. This scheme is appropriate for Voice over IP applications [28].

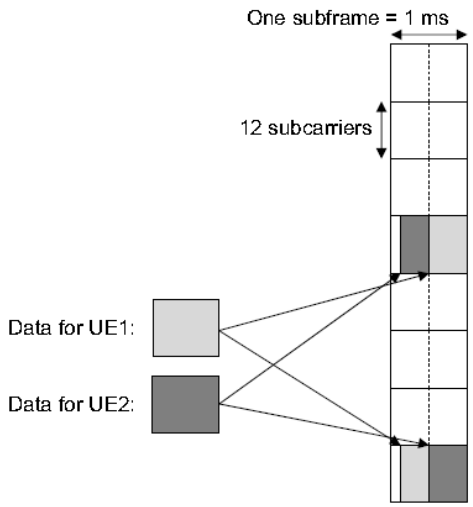

Figure 5.10 Frequency distributed data mapping [28]

Besides data bearing, PDSCH is used to convey dynamic broadcasting in formations that are not carried by PBCH. Also, since there is no specific physical channel associated with paging information, PDSCH is used for this purpose as well. In this case, a paging indicator is carried by PDCCH and each UE monitors PDCCH for its paging indicator; however, paging information is carried by resource blocks in PDSCH indicated by PDCCH [28].

5.3.1.6 **PMCH**

Multimedia Broadcast and Multicast Services (MBMS) are available in later releases of LTE such as Release 9 and 10. However the physical channel structure is defined for future use. MBMS enables a set of eNBs to transfer information simultaneously for a

given duration. This transmission is known as Multicast/Broadcast over a Single Frequency Network (MBFSN) and uses a longer cyclic prefix to cover the propagation delay in UE resulting from multiple eNB transmitted signals. Therefore, MBFSN appears to UE as a transmission from a single large cell and improves the signal-to-interference noise ratio. Since the operation of data transmission is different from that of MBFSN, UE should have a separate channel estimate for MBSFN reception; therefore normal reference signal is not mixed with the MBSFN reference signal in the same subframe and transmission of PDSH and PMCH in the same subframe is not possible.

While PDSCH transmission is based on normal cyclic prefix and PMCH transmission needs to use the extended cyclic prefix, the first two OFDM symbols assigned for PDCCH uses the normal cyclic prefix in PMCH transmission.

5.3.1.7 **Reference Signals**

Reference signals (RSs) in LTE are used for channel estimation and are sent on particular resource elements by a predefined structure. RSs are classified into three categories:

- Cell-specific RSs that are available to all UEs in the cell and also known as common RSs.
- UE-specific RSs that are used for specific UEs
- MBSFN-specific RSs that are used for MBFSN operations

5.3.1.7.1 ***Cell-Specific RS***

In order to achieve the minimum mean square error estimate of the channel and optimize the diamond shape in the time frequency plane, the arrangement of RS in LTE is uniform in frequency and time domain [28].

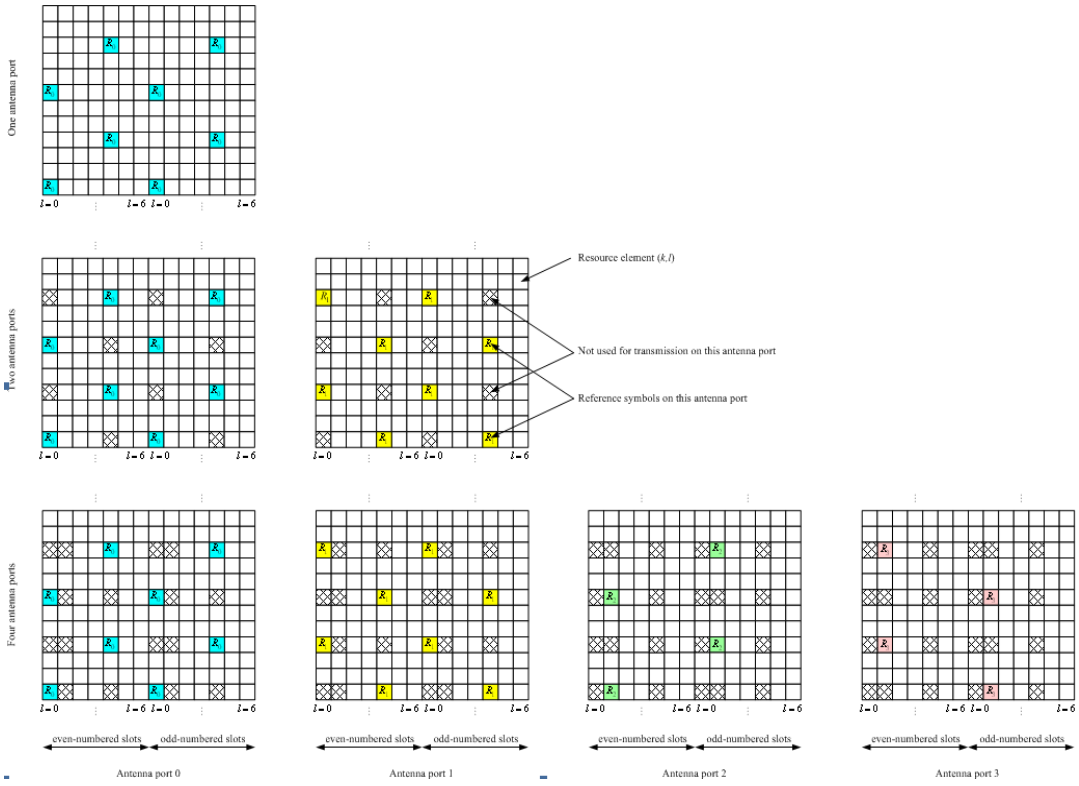

Figure 5.11 Mapping of cell specific reference signal (normal cyclic prefix) [6].

Figures 5.11 and 5.12 demonstrate a cell-specific RS arrangement for a normal and extended cyclic prefix, respectively, in the case of one, two and four antenna ports. As shown in these two figures, a reference symbol is transferred every six subcarriers in the frequency domain. Moreover, in one RB there is one reference symbol every three

subcarriers. This structure depends on the coherence bandwidth which is 20 kHZ and 200 kHz for 90% and 50%, respectively. Therefore, 45 kHz of spacing allows resolving the expected frequency domain variations [28]. In time domain the required spacing can be calculated considering the minimum sampling rate based on Nyquist's sampling criteria

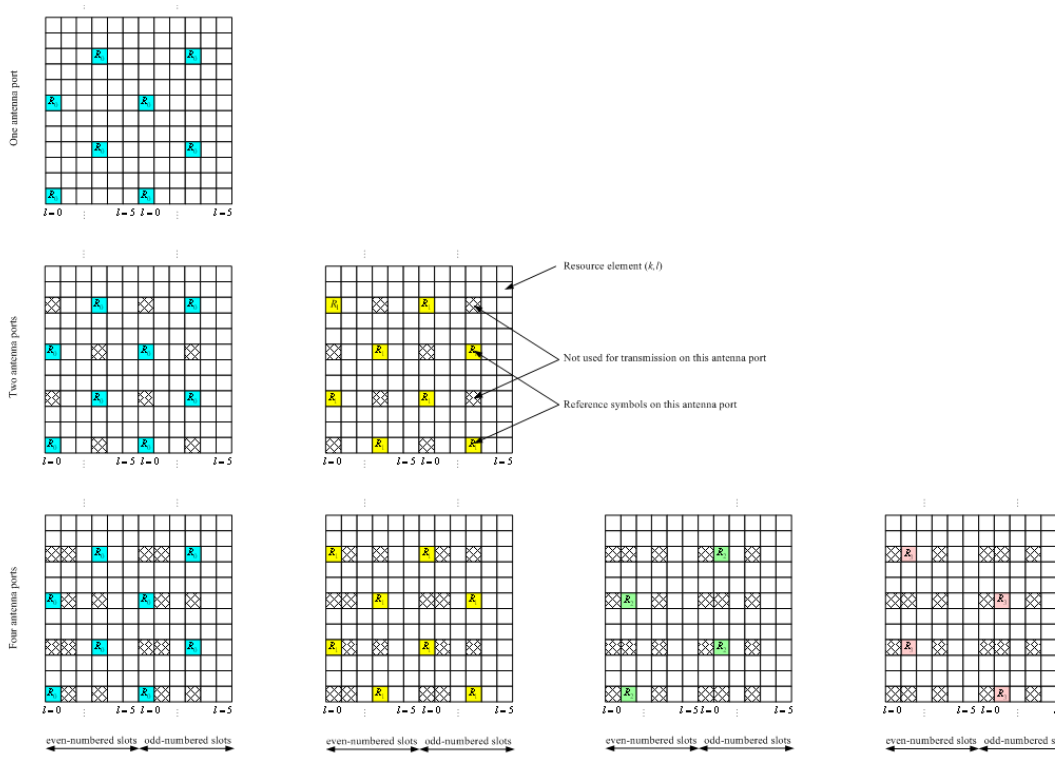

Figure 5.12 Mapping of cell specific reference signal (normal cyclic prefix) [6].

$T_c = 1/ (2*f_d)$. f_d is known as dopler shift and can be calculated by $f_d = (f_c * v) / c$, where f_c is the carrier frequency that equals 2 GHz for LTE, v is the highest speed for LTE supporting mobility (500 km/h), and c is the speed of light ($3*10^8$). By calculating f_d = 950 Hz, T_c will be 0.5 ms, which leads to two reference symbols in one slot for accurate channel estimation [28]. The modulation for all types of reference signals is based on QPSK.

5.3.1.7.2 ***UE-specific RS***

The main advantage of using a UE-specific reference signal is to enable beam forming for specific UEs. Therefore eNB can use a correlated array of antennas rather than other

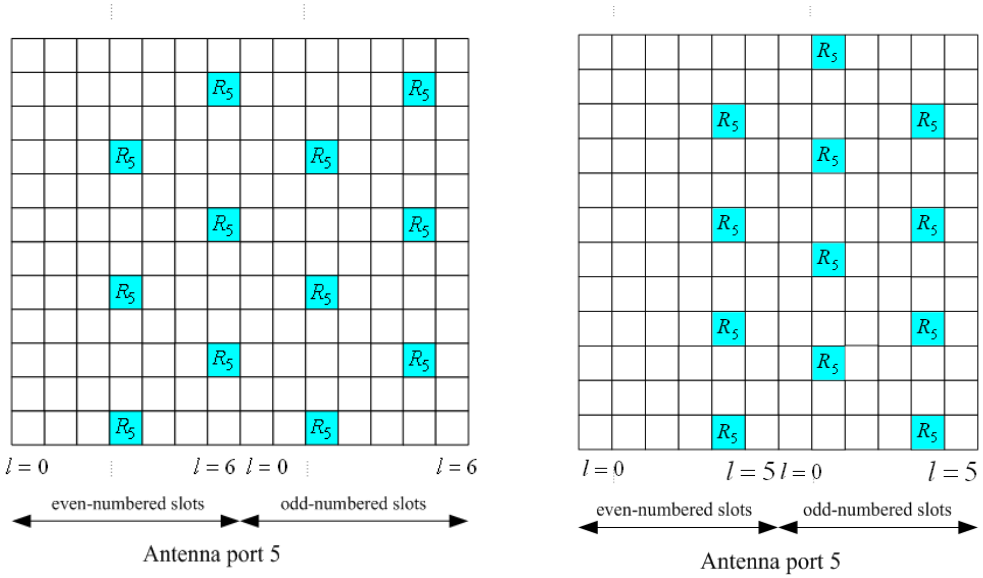

Figure 5.13 Mapping UE-specific reference signal for normal and extended cyclic prefix [6].

antenna ports to establish a beam to UE that yields to different channel response. For channel estimation and data demodulation, a different reference signal is required beside the cell specific reference signal. Figure 5.13 shows the allocation of reference symbols for normal and extended cyclic prefix [28].

5.3.1.8 **Synchronization Signals**

Before initiating the communication with eNB, UE should be able to determine time and frequency in order to correctly demodulate received data and transmit data with the right time and frequency parameters. Moreover, the start position of the symbol, carrier frequency synchronization, and sampling clock synchronization is needed by UE. In LTE

there are two synchronization signals that are designed for mentioned purposes: Primary Synchronization Signal (P-SS) and Secondary Synchronization Signal (S-SS).

5.3.1.8.1 ***P-SS***

P-SS provides slot timing information and Physical layer ID for UE. The channel detection method for P-SS is coherent. P-SS takes advantage of the frequency-domain Zadoff-Chu sequence to generate 62 symbols for transmission. For FDD operations associated with the frame structure type1, P-SS is mapped to the last OFDM symbol in slot0 and 10, and the subcarrier indices are indicated as

$$k = n - 31 + (NRB_{dl} * NSC_{rb}) / 2 \qquad n = 0, 1, 2, \ldots, 61$$

In case of TDD operation (frame structure type 2), P-SS is mapped to the third OFDM symbol in subframe 1 and 6 and the subcarrier indices can be determined as

$$k = n - 31 + + (NRB_{dl} * NSC_{rb}) / 2 \qquad n = -5,-4,\ldots,-1, 62, 63,\ldots, 66$$

5.3.1.8.2 ***S-SS***

S-SS utilizes UE with the information of cell ID, cyclic prefix length, and whether the eNB is working based on TDD or FDD operations. Both coherent and non-coherent techniques can be used for S-SS detection. Using a concatenated sequence, S-SS consists of 62 symbols to be transmitted over subcarrier indices:

$$k = n - 31 + (NRB_{dl} * NSC_{rb}) / 2 \qquad n = 0, 1, 2, \ldots, 61$$

for frame structure type 1 OFDM indix equals to $NSB_{dl} - 2$ in slot 0 and slot 10; however, in frame structure type2 S-SS is transmitted in OFDM symbol (NSB_{dl} -1)th of slots 1 and 11.

Based on previous discussion of downlink physical channels and synchronizations and reference signals, a possible mapping of physical channels and reference signals is shown in Figure 5.6 for 20 MHz system bandwidth.

5.3.2 **Uplink structure and specifications**

Uplink information, like downlink transmission, is carried out through physical channels listed below:

PUSCH: Physical Uplink Share Channel

PUCCH: Physical Uplink Control Channel

PRACH: Physical Random Access Channel

Reference signals supported in uplink transmission are:

D-RS-PUSCH: Demodulation RS associated with PUSCH

D-RS-PUCCH: Demodulation RS associated with PUCCH

S-RS: Sounding Reference Signal

Similar to downlink parameters, the following parameters are defined and used for uplink:

k: frequency domain index (subcarrier index)

l: time domain index (SC-FDMA symbol index)

NRB_{ul} : number of resource blocks in uplink

NSB_{ul} : number of SC-FDMA symbols for one resource block in uplink

NSC_{rb}: number of subcarriers in resource block

REG: Resource Element Group. A set of four physical Resource Elements

5.3.2.1 **Demodulation Reference Signals**

D-RS-PUSCH and D-RS-PUCCH are two uplink reference signals used for channel estimation and coherent demodulation. This type of reference signal occupies the same bandwidth as its associated physical channel.

5.3.2.1.1 ***D-RS-PUSCH***

This reference signal is associated with uplink data and is mapped to the 4th SC-FDMA symbol for a Normal cyclic prefix and the 3rd SC-FDMA signal for an extended cyclic prefix. Table 5.9 shows the number of DM-RS-PUSCH assigned for different transmission bandwidths.

Table 5.9 Number of resource elements assigned for D-RS-PUSCH in one radio frame

	NRBul					
	6	15	25	50	75	100
D-RS-PUSCH	1200	3360	5760	11760	17760	23760

5.3.2.1.2 *D-RS-PUCCH*

The location of this reference signal depends on the PUCCH format, which will be discussed later in this chapter. Table 5.10 shows the set of values for SC-FDMA symbols for D-RS-PUCCH mapping.

Table 5.10 Number of SC-FDMA symbols and location of D-RS-PUCCH

	SC-FDMA symbol index in the slot used for PUCCH transmission	
PUCCH format	Normal Cyclic Prefix	Extended Cyclic Prefix
1, 1a, 1b	2, 3, 4	2,3
2	1, 5	3
2a, 2b	1, 5	N/A

5.3.2.2 **S-RS**

This reference signal is mainly used for channel quality estimation for frequency selective scheduling or providing initialization and set-up functions for UEs that are not scheduled. These functions may include the modulation and coding scheme, initial power and timing information, etc. The location of S-RS is indicated by srsConfiguration parameter that is 4 bits defining 15 sets of subframes. SRS is mapped to the last SC-FDMA symbol in subframes. The main point is that PUSCH data cannot be transmitted in the SC-FDMA symbol that SRS is transmitted with. There are two modes of SRS transmission request that eNB may request. This configuration is determined by a 1 bit ‘duration’ parameter that indicates whether the SRS transmission is single or periodic. In periodic scheme, UE transmits SRS in a given period of time until terminated. This period can be 2, 5, 10, 20, 40, 80, 160, or 320 ms. This period, along with the subframe offset used for periodic SRS transmission, is indicated by a 10-bit parameter known as ‘srsConfiguration’.

5.3.2.3 **PUCCH**

This physical channel conveys the control information that is not related to uplink data. One of the control information, CQI, is 20 bits [19]. The CQI information that is transmitted by PUCCH is periodic CQI reporting.

HARQ information is an ACK/NACK response to downlink data packets and depends on the number of codewords transmitted through one subframe (1 or 2 codewords), which can be 1 or 2 bits. PUCCH also includes Scheduling Request (RS) information that is associated with the lack of enough resources to send uplink data. Based on the information that this physical channel contains, there are six formats for this channel as listed in Table 5.11.

Table 5.11 PUCCH formats [6]

PUCCH format	Modulation Scheme	Number of bits per Subframe	Information
1	N/A	N/A	Scheduling Request
1a	BPSK	1	HARQ
1b	QPSK	2	HARQ
2	QPSK	20	CQI
2a	QPSK and BPSK	21	CQI and HARQ
2b	QPSK	22	CQI and HARQ

The allocation of PUCCH is based on the frequency diversity that means PUCCH is mapped to the pair of RBs in the opposite edge of the system bandwidth. Depending on PUCCH format mapping to the resource elements is shown in Figure 5.14 [28].

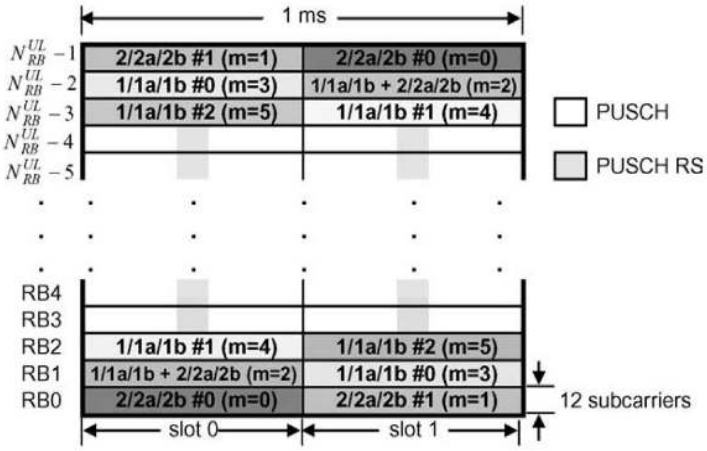

Figure 5.14 PUCCH resource block allocation [28]

Based on this figure, the number of resource elements assigned for PUCCH is fixed based on the given format and does not depend on the system bandwidth.

5.3.2.4 **PUSCH**

This channel carries data for different UEs through the resource elements that are not allotted to PUCCH, DM-RS, and SRS. The modulation scheme for this channel can be QPSK, 16-QAM, or 64-QAM. Table 5.12 presents the number of resource elements available for PUSCH transmission.

Table 5.12 PUSCH resource elements

	NRBul					
	6	15	25	50	75	100
PUSCH REs	5760	18720	33120	69120	105120	141120

5.3.2.5 **Physical Layer Outline**

Based on the information stated in Sections 5.3.1 and 5.3.2, a LTE physical channel outline can be presented for FDD downlink and uplink and TDD operations. Figure 5.15 shows downlink allocation for physical channels and reference signals for the FDD

scheme. It is assumed that four antenna ports are supported. In Figure 5.17, uplink physical channels and reference signals are illustrated supporting format 2/2a/2b of PUCCH. The TDD scheme in mode 0 is demonstrated in Figure 5.16. These three figures are based on 20 MHz system bandwidth.

Figure 5.15 FDD Downlink physical layer configuration for 20 MHz system bandwidth and 4 antenna ports.

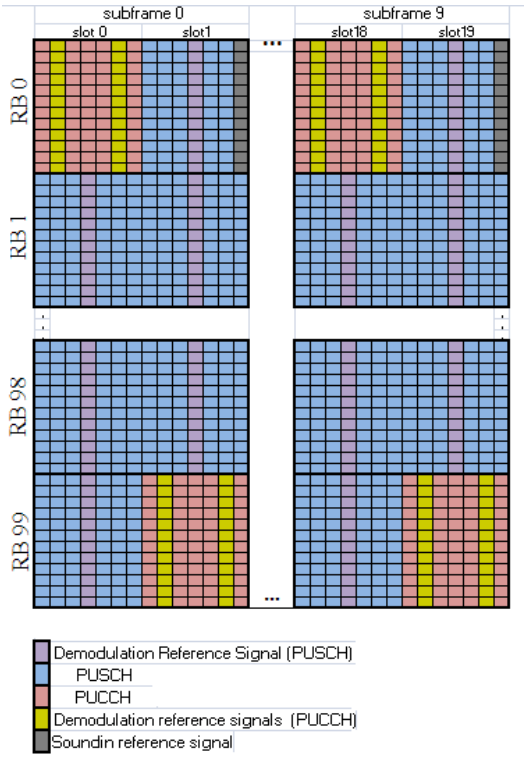

Figure 5.17 FDD Uplink physical layer configuration for 20MHz system bandwidth and 2/2a/2b PUCCH scheme.

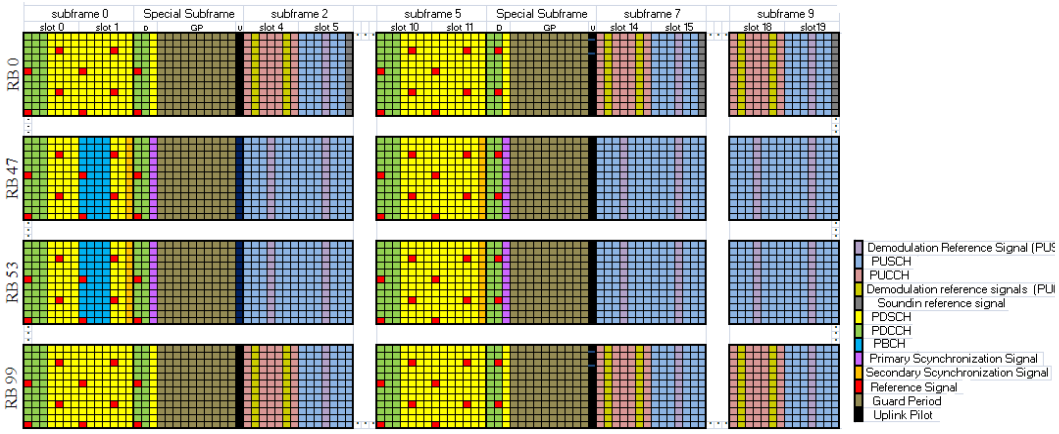

Figure 5.16 TDD physical layer configuration for 20MHz system bandwidth in case of mode 0.

5.4 Channel Coding and Rate Matching

5.4.1 Channel Coding

The channel coding for data channels in LTE uses turbo code, whose performance is close to the Shannon limit. A turbo encoder used in LTE consists of two convolutional concatenated encoders that are connected to each other by an interleaver, as shown in Figure 5.18. As we can consider the code rate of this turbo coder is 1/3 and two generated polynomials are G0= [1011] and G1= [1101].

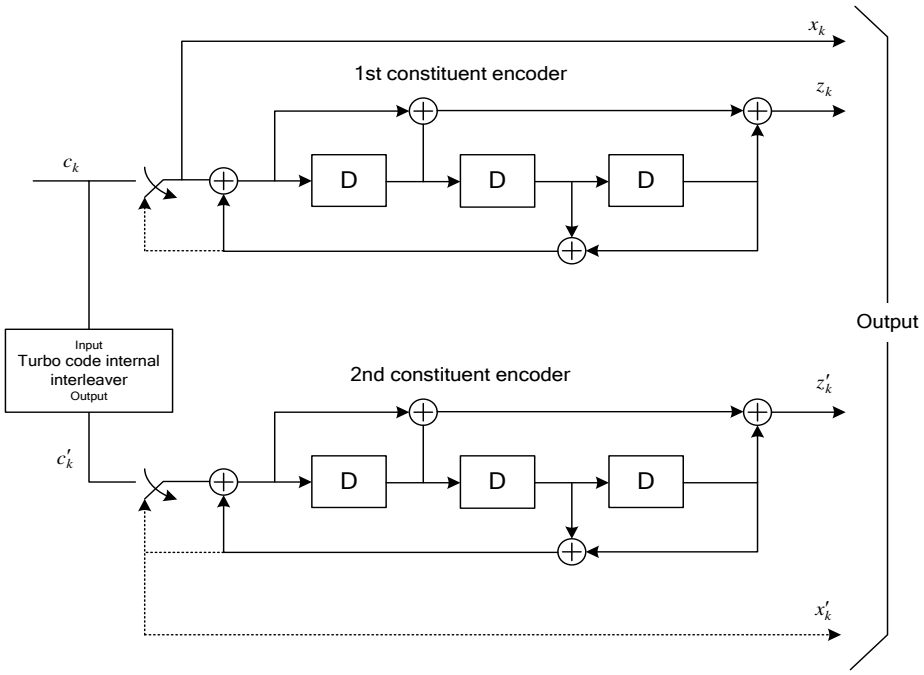

Figure 5.18 LTE turbo coder [6]

5.4.2 Interleaver

From two candidates of interleaver for LTE, Quadratic Permutation Polynomial (QPP) and Almost Regular Permutation (ARP), QPP was selected. QPP satisfies high data rates

since it requires less memory and provides more parallelism factors. Assuming that the block size information is indicated by K, the output index is shown as i ($0 \leq i \leq K-1$), and the input index is π (i). The QPP polynomial is defined as:

$$\pi (i) = (f_1 i + f_2 i^2) \bmod K$$

f_1 and f_2 are coefficients defined as :

f_1 is relatively prime to block size K and all prime factors of K also factor f_2

For better performance of the QPP interleaver, inverse polynomials should be low-degree. The value for LTE QPP inverse polynomial interleaver is 4.

One of the key features of QPP interleavers is that they are maximum connection-free, and hence they provide maximum flexibility in supported parallelism. Therefore every factor of K is a supported parallelism factor. For instance, if K= 1024, supported parallelism factors are: [1, 2, 4, 8, 16, 32, 64, 128, 256, and 512].

5.4.3 **Rate Matching Algorithm**

From the rate 1/3 output of the turbo coder, the Rate Matching (RM) algorithm selects bits for transmission via puncturing or repetition. The LTE rate matching approach is a circular buffer that provides a variety of code rates through generating different puncture patterns. Figure 5.19 demonstrates the circular buffer RM.

The output of the turbo encoder is three K-length streams: systematic bits, Parity0 and Parity1. Trellis termination is 12 bits that is divided to each stream evenly, such that the length of each code word is K+4. The turbo coder code rate is a bit less than 1/3. Each

stream has a sub-block interleaver, in which K+4 bits are written to a matrix with 32 columns row by row. Based on a predefined pattern, inter column permutation is applied and then bits are read out column by column.

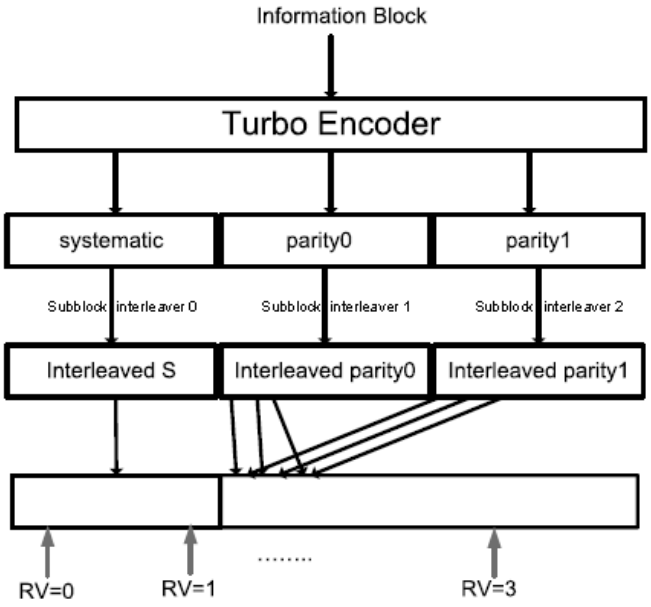

Figure 5.19 Rate matching Algorithm based on Circular Buffer [28]

After this stage there are three streams of length R= 32*Number of rows. The circular buffer is filled with R bits of interleaved systematic stream (indices 0 to k). Indices R+2k and R+2k+1 are placed with R bits of parity 0 and parity 1 respectively. Therefore the circular buffer size is 3R and for desired code rate N coded bits should be selected. The selection of N coded bits can be started from any point in 3R size buffer. Circular buffer term refers to this technique that if the end of the buffer is reached bit selection continues from the beginning of the buffer [30].

The rate matching algorithm contains different subsets of coded bits called Redundancy Version (RV), which points to different locations of the circular buffer.

Chapter 6. **Proposed Performance Study**

In this chapter, physical layer data throughput is calculated accurately for different scenarios. In order to determine physical layer performance we need to calculate the total physical resources available for different bandwidths of uplink and downlink transmission. On the other hand, we need to determine how many physical resources are associated with overhead. Different physical channels and reference signals are described in section 5.3 (Physical Channels and Reference Signals) for downlink and uplink transmission, and how these channels are allocated and multiplexed.

Different values are mentioned for LTE physical layer throughput as discussed in chapter 7 (Modeling and Simulation); however, some materials presented the physical layer throughput as 100 Mbps, 150Mbps and 300 Mbps for 1, 2 and 4 antenna ports respectively. In this study, based on the parameters of physical layer proposed in 3GPP standard Release 8, various scenarios are considered for physical layer throughput. Based on system bandwidth (1.4 to 20 MHz), number of antenna ports (1, 2, or 4), number of OFDM symbols assigned for PDCCH (1, 2, or 3 symbols per subframe), code rate (0.33 to 0.92), and modulation scheme (QPSK, 16-QAM, or 64-QAM) different throughput values can be addressed.

For downlink transmission, eNB decides which modulation and code rate to use based on the CQI feedback that is transmitted by UE. eNB also can estimate the code rate and modulation scheme by using the sounding reference signal (SRS). So LTE takes

advantage of the Adoptive Modulation and Coding (AMC) technique which is based on the signal quality, a specific modulation scheme and code rate that is selected for data transmission. AMC is constant for the resource blocks allocated for a given user; however, different users can have different modulation and code rates (time domain supported AMC). Also, for multi-antenna transmission, each layer can use independent modulation and coding schemes.

Beside PDSCH as discussed in section 5.3 (Physical Channels and Reference Signals), there are other physical channels that provide information for the upper layer, but however this information is mainly control and broadcast information. In some material this kind of information is considered for calculation of maximum throughput. In this study, however, throughput calculation is based on data channels for uplink and downlink and does not include any kind of control information.

6.1 FDD Downlink Throughput

PDCCH can occupy one to four OFDM symbols in downlink, and therefore PDCCH overhead varies from 2.3% (one OFDM symbol in the case of four antenna ports and 20MHz band width) to 27% (four OFDM symbols in the case of one antenna port and 1.4MHz band width). Reference signal is mapped to resource elements based on the number of antenna ports. For one antenna port, reference signal overhead is 4.7%; this overhead increases to 9.5% and 14% in the case of two and four antenna ports, respectively. Synchronization signal overhead for both P-SS and S-SS can be considered 1.4% (for 1.4 MHz bandwidth) and 0.085% (for 20 MHZ bandwidth) as minimum and

maximum values. The overhead related to PBCH can be 2.7% to 0.14% based on channel bandwidth.

The number of Physical Downlink Share Channels (PDSCH, see section 5.3 (Physical Channels and Reference Signals) for more information) resource elements (the smallest entity of data transmission, see section 5.2 (Physical Layer General Description) for more information) is shown in Figures 6.1 to 6.3 for one, two and four antenna ports, respectively. It should be noted that for six resource blocks the minimum and maximum OFDM symbols occupied by PDCCH are two and four, respectively, and in Figures 6.1 to 6.3 highlighted values for six resource blocks refer to four OFDM symbols assigned to PDCCH.

The maximum physical layer throughput can be calculated by applying the channel coding and modulation schemes to these resource elements available for data transmission. For example, the maximum throughput in the case of one antenna port, one OFDM symbol assigned for PDCCH, 64-QAM modulation and 0.85 code rate, is 75.31 Mbps. If two antenna ports are used in this scenario, the maximum throughput reaches 144.595 Mbps. The maximum throughput of four antenna ports and 0.92 code rate in the previous scenario is 299.122 Mbps.

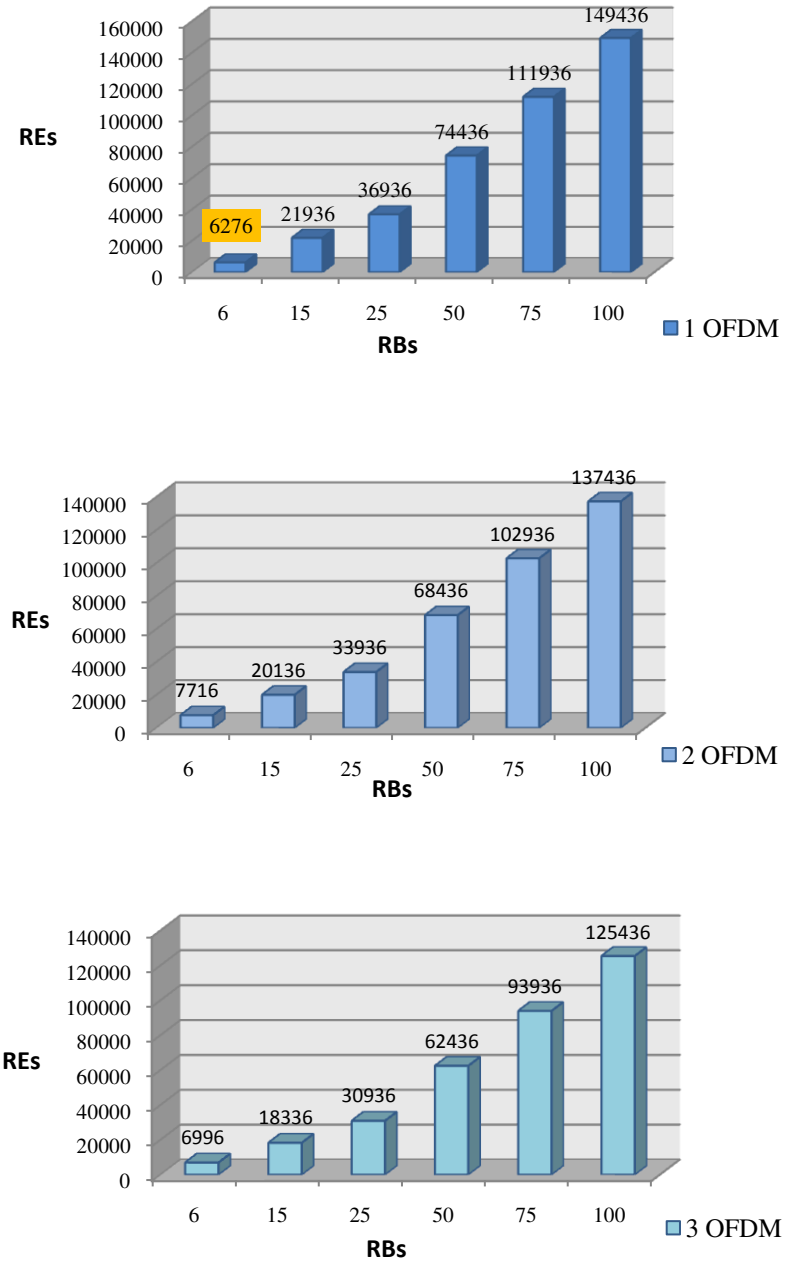

Figure 6.1 PDSCH REs in1 radio frame and 1 Tx antenna, FDD. PDCCH occupies 1,2,3, or 4 OFDM symbols

Highlighted value indicates 4 OFDM symbols instead of one for PDCCH

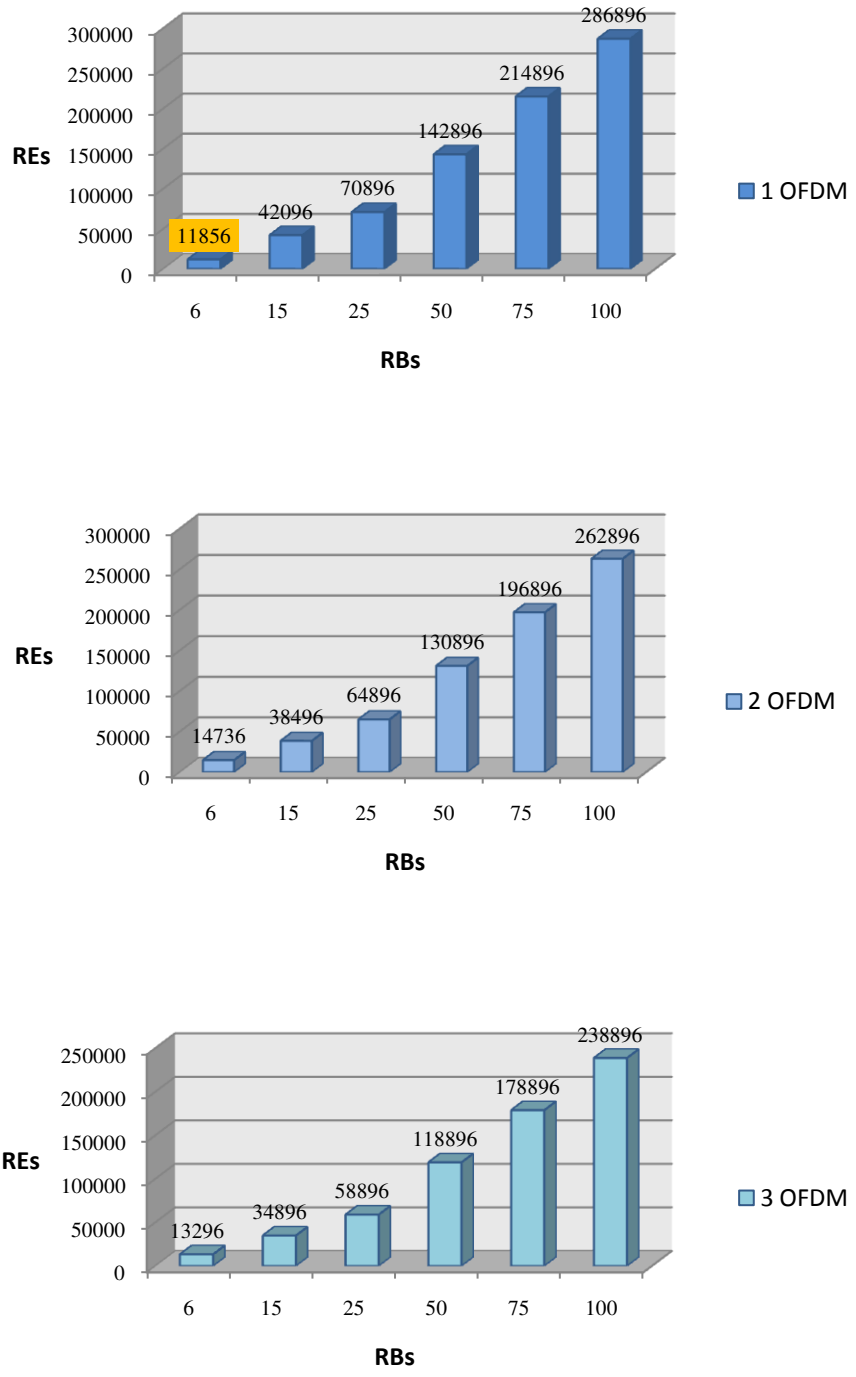

Figure 6.2 PDSCH REs in1 radio frame and 2 Tx antennas, FDD. PDCCH occupies 1,2,3, or 4 OFDM symbols

Highlighted value indicates 4 OFDM symbols instead of one for PDCCH

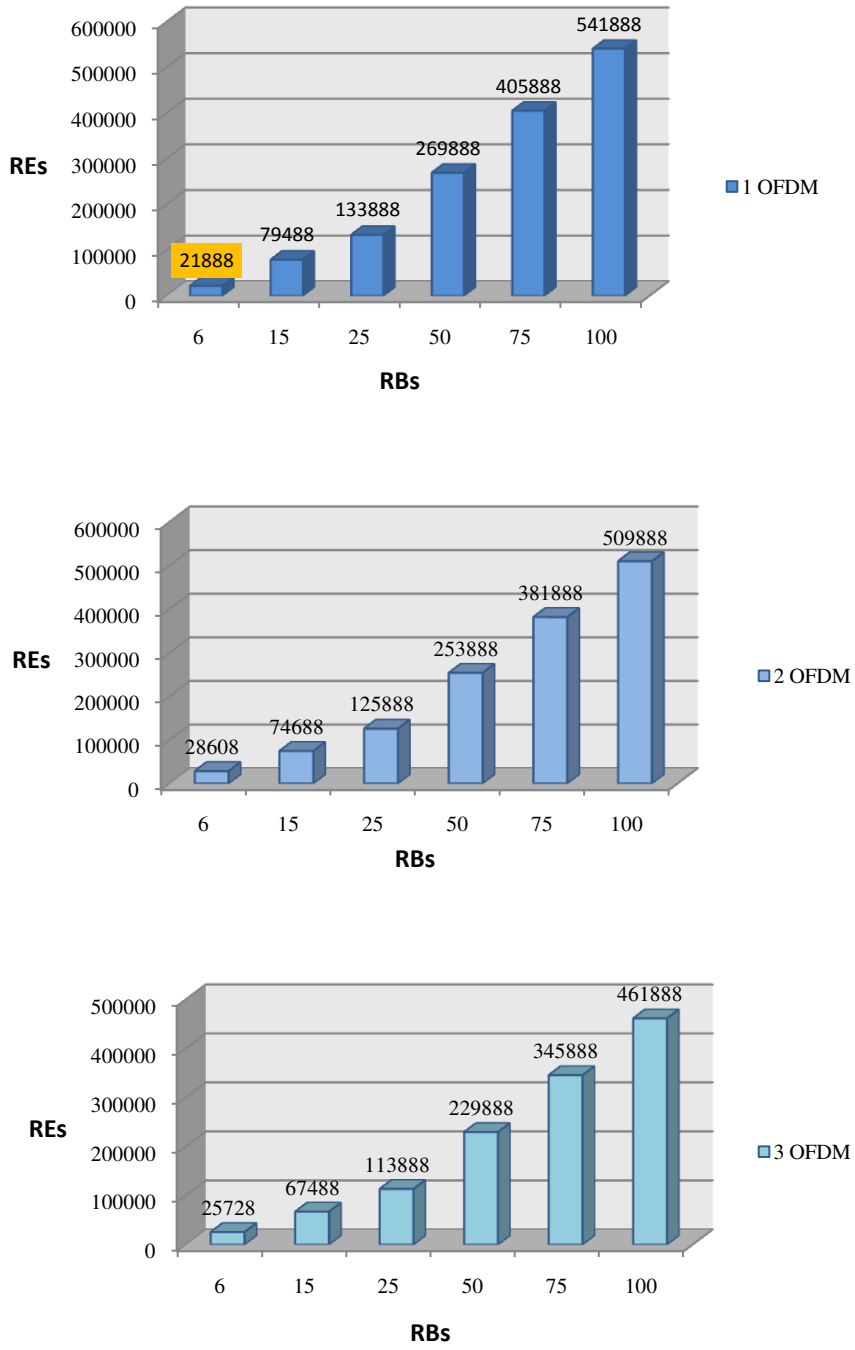

Figure 6.3 PDSCH REs in1 radio frame and 4 Tx antennas, FDD. PDCCH occupies 1,2,3, or 4 OFDM symbols

Highlighted value indicates 4 OFDM symbols instead of one for PDCCH

6.2 FDD Uplink Throughput

In Uplink transmission excluding control information and reference signals overhead (PUCCH, CQI, ACK/NACK: 1.5% to 25%, DM-PUCCH: 4.7% to 0.028%, DM-PUSCH: 11% to 14%, and sounding RS: 1.1% to 0.007%), the resource elements assigned to PUSCH is presented in Figure 6.4 and the maximum throughput of uplink transmission can be addressed by applying the channel coding and modulation scheme. for instance in case of 20 MHZ system bandwidth, 64-QAM modulation, and applying code rate of 0.85 the maximum through put of uplink will be 71.97 Mbps.

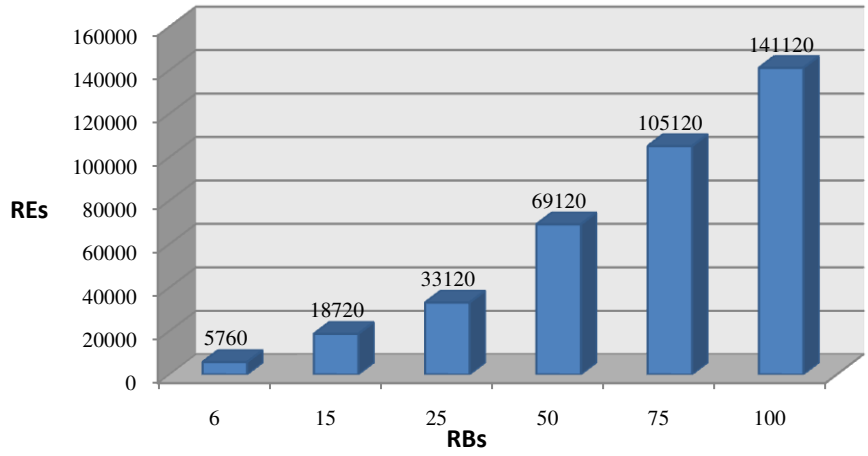

Figure 6.4 PUSCH REs in1 radio frame, FDD.

6.3 TDD Uplink and Downlink Throughput

In TDD operation, there are seven different configurations for transmission of uplink and downlink data. MOD 0 is the configuration that assigns the most number of

subframes to uplink transmission (total of six subframes); however, in MOD 5 the most number of subframes are allotted to downlink transmission (8 subframes). The maximum PDSCH and PUSCH resource elements can be achieved with MOD 5 and MOD 0 respectively. Figures 6.5 to 6.7 show the PDSCH resource elements in mode 5 when 1,2, or 3 OFDM symbols are assigned to PDCCH in different antenna port schemes. Figures 6.8 to 6.10 show the PDSCH resource elements in Mode 0 for different antenna schemes and different OFDM symbols assigned to PDCCH.

Therefore, as presented in Figure 6.7, the maximum throughput of PDSCH in TDD operation can be achieved when using mode 5, 4 antenna transmission, and the least control information (1 OFDM for PDCCH). In this case, for 64-QAM of data modulation, and 0.92 code rate, the maximum throughput is 239.382 Mbps. In the same scenario for two antenna transmission, PDSCH throughput is 126.730 Mbps.

Figure 6.11, shows the resource elements for PUSCH in mode 0 and mode5. Due to the fact that mode 0 contains the most number of subframes for uplink data transmission, hence PUSCH throughput is 431.827 assuming 64-QAM data modulation, 0.85 code rate and 20 MHz bandwidth.

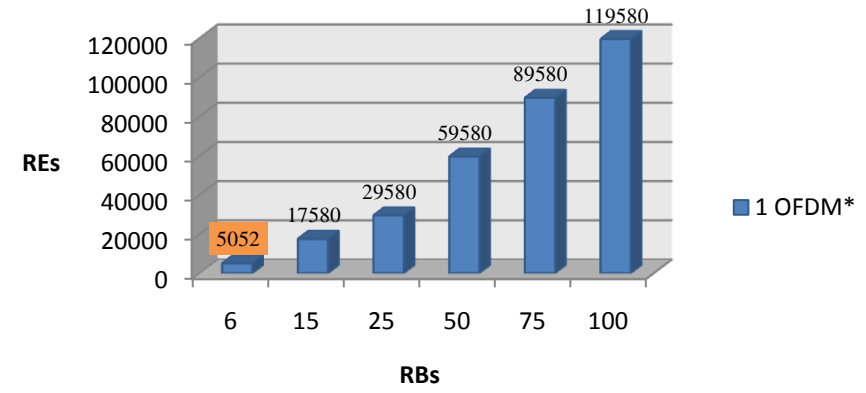

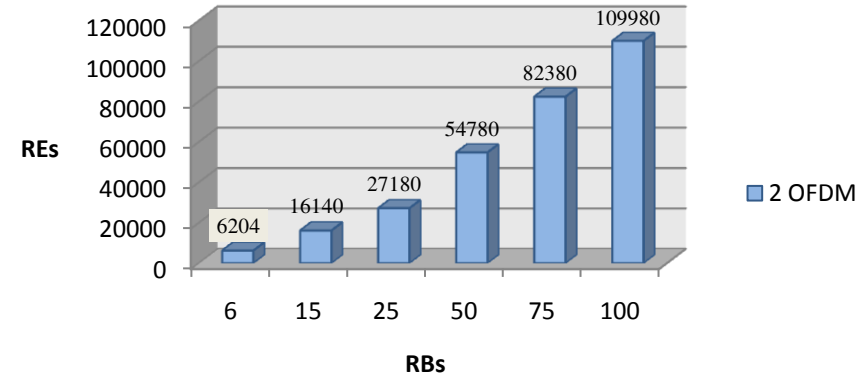

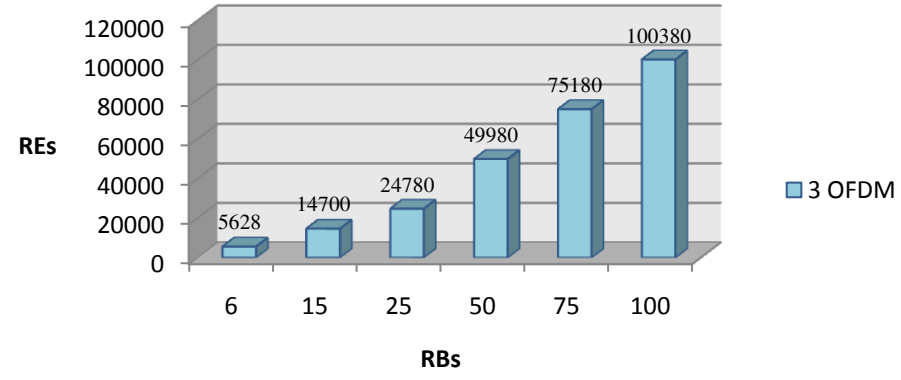

Figure 6.5 PDSCH REs in1 radio frame and 1 Tx antenna, TDD mode 5. PDCCH occupies 1,2,3, or 4 OFDM symbols.

Highlighted value indicates 4 OFDM symbols instead of one for PDCCH

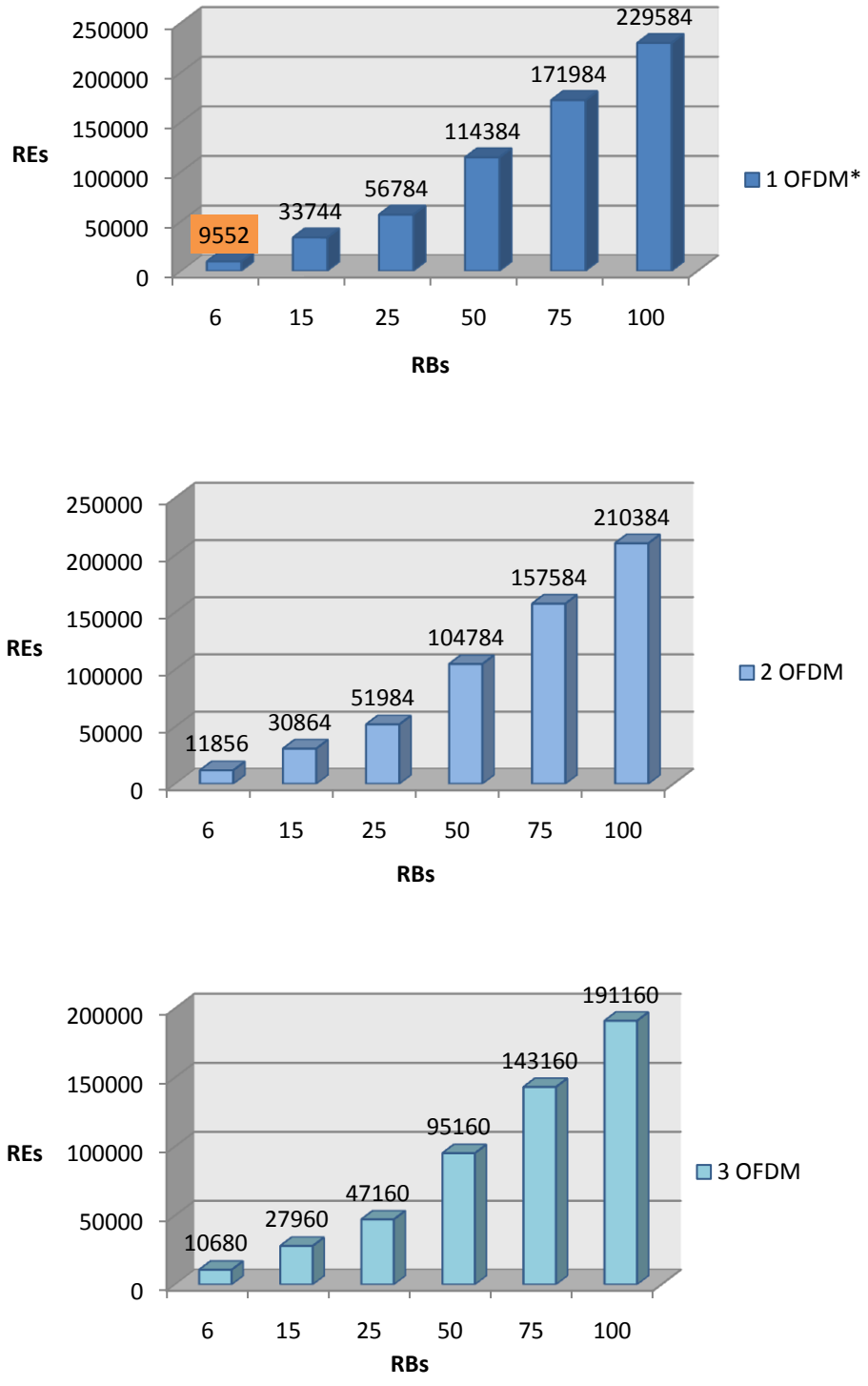

Figure 6.6 PDSCH REs in1 radio frame and 2 Tx antennas, TDD mode 5. PDCCH occupies 1,2,3, or 4 OFDM symbols.

Highlighted value indicates 4 OFDM symbols instead of one for PDCCH

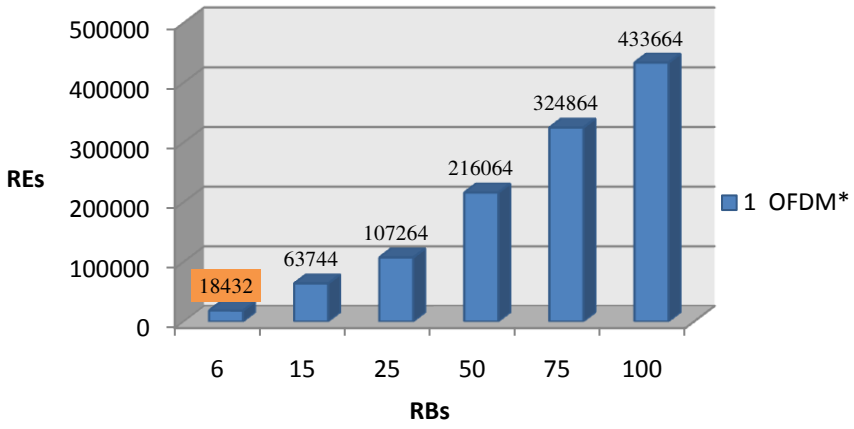

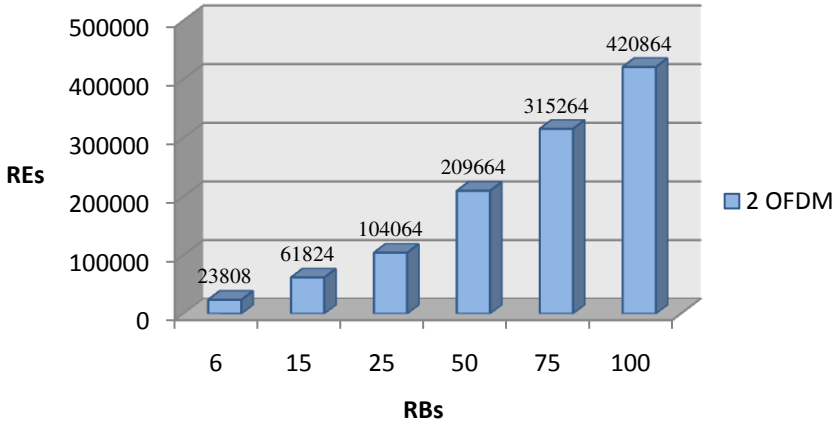

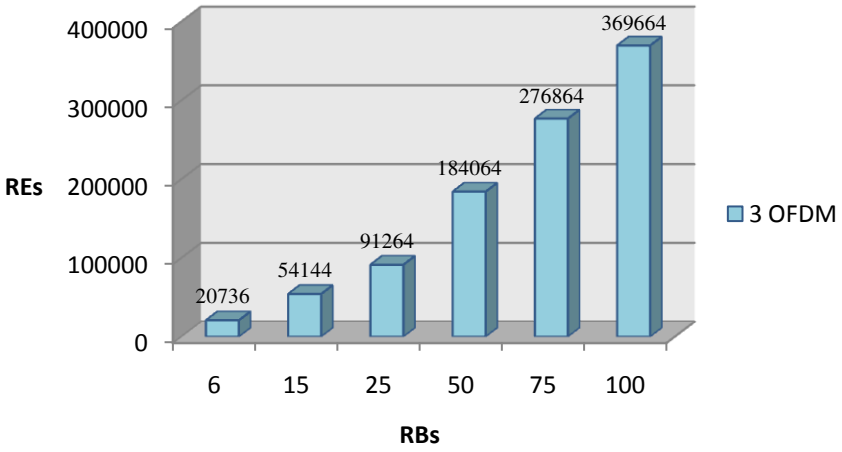

Figure 6.7 PDSCH REs in1 radio frame and 4 Tx antennas, TDD mode 5. PDCCH occupies 1,2,3, or 4 OFDM symbols.

Highlighted value indicates 4 OFDM symbols instead of one for PDCCH

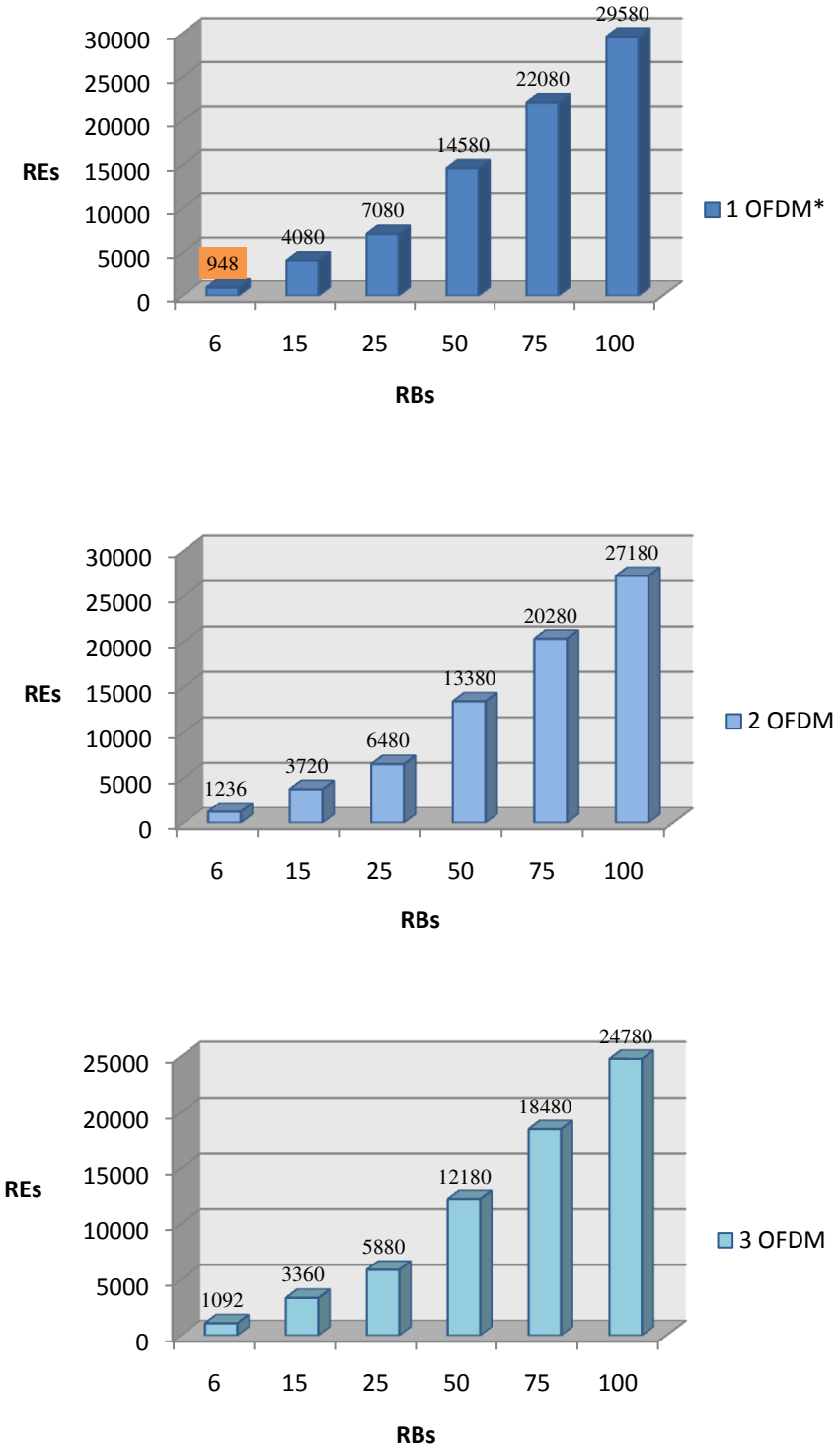

Figure 6.8 PDSCH REs in1 radio frame and 1 Tx antenna, TDD mode 0. PDCCH occupies 1,2,3, or 4 OFDM symbols.

Highlighted value indicates 4 OFDM symbols instead of one for PDCCH

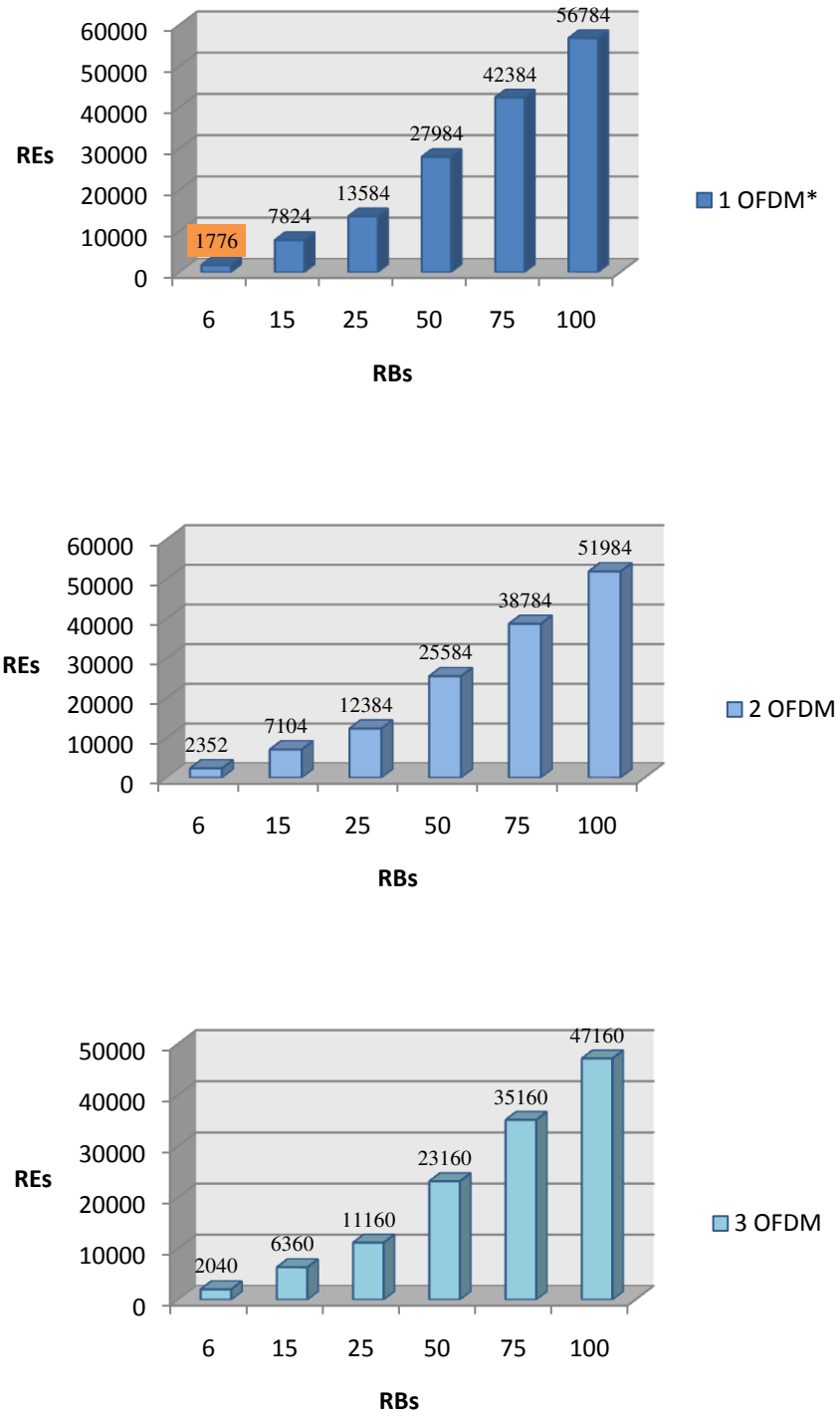

Figure 6.9 PDSCH REs in1 radio frame and 2 Tx antennas, TDD mode 0. PDCCH occupies 1,2,3, or 4 OFDM symbols.

Highlighted value indicates 4 OFDM symbols instead of one for PDCCH

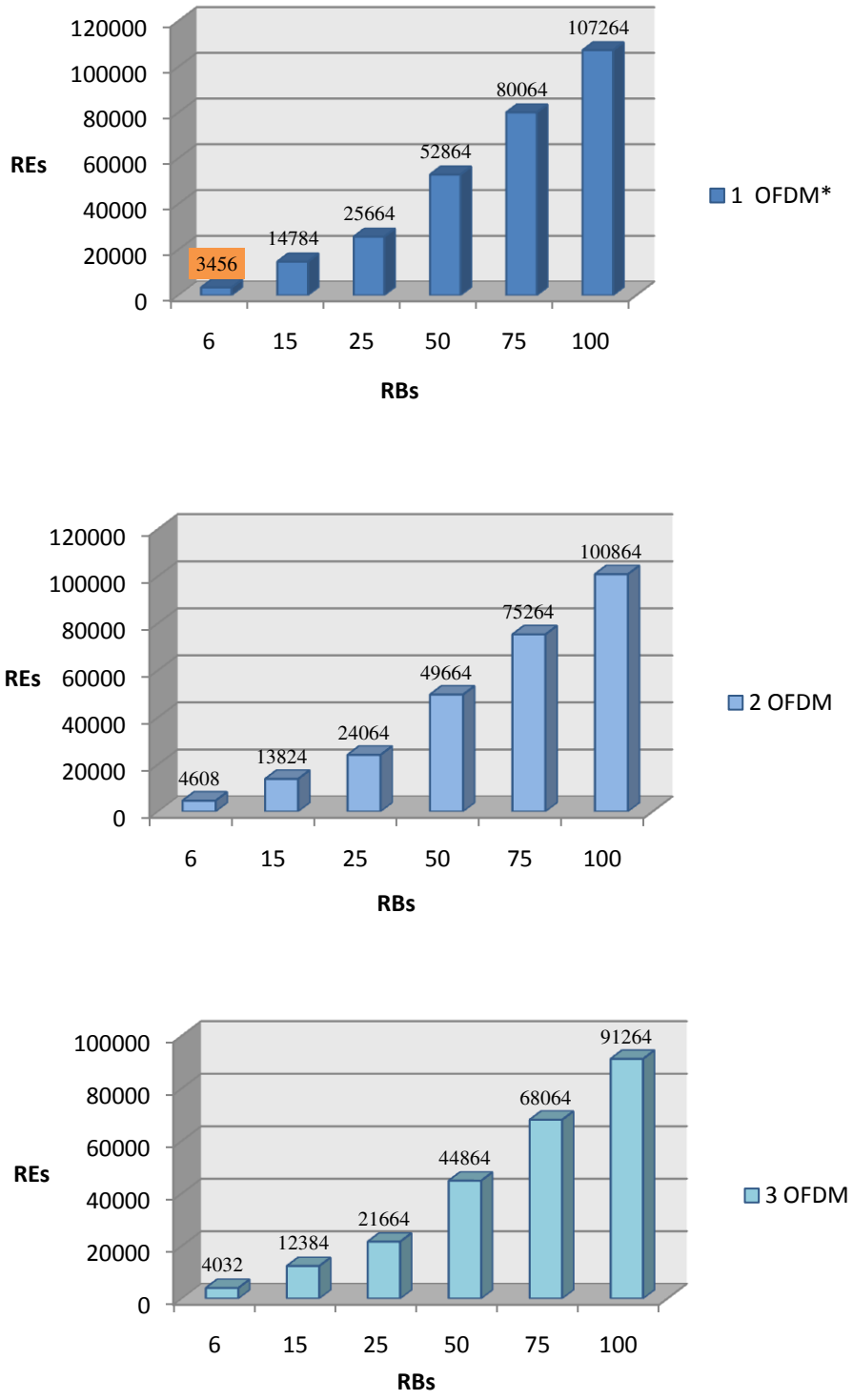

Figure 6.10 PDSCH REs in1 radio frame and 4 Tx antennas, TDD mode 0. PDCCH occupies 1,2,3, or 4 OFDM symbols.

Highlighted value indicates 4 OFDM symbols instead of one for PDCCH

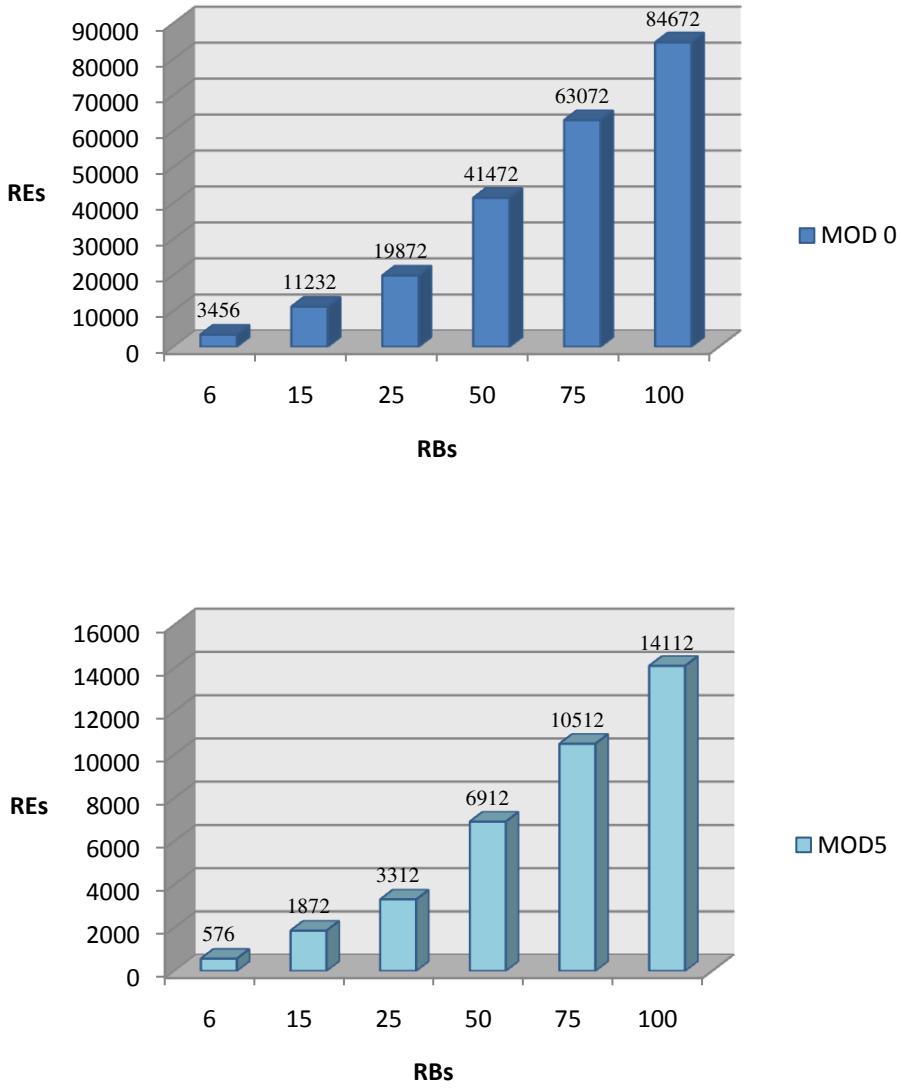

Figure 6.11 PUSCH REs in1 radio frame and 1 Tx antennas, TDD MOD0 and MOD6.

Based on all of the mentioned scenarios, we know the maximum data that can be sent through the channel. However due to channel noise, interference, distortion, etc. the number of received correct bits is less than what is transmitted. Altered bits are called bit errors, and the ratio of error bits to total number of transferred bits is known as Bit Error

Rate (BER). BER values can be gained vs. SNR (Signal-to-Noise Ratio) to calculate the throughput value in different SNR points the maximum data bits that can be received without error by a given SNR point can be indicated. The results of these calculations and details are provided in Chapter 7 (Modeling and Simulation) and Chapter 8 (Results and analysis).

Chapter 7. **Modeling and Simulation**

This chapter describes the simulation and modeling approach used in this study. Results are based on link level simulation. In the first step the description of physical layer procedure for uplink and downlink is provided, followed by the simulation parameters and values.

Figure 7.1 shows the steps that an input sequence of bits (one transport block) is going through to finally become an OFDM signal for a downlink data channel. Based on this figure 24 bits of CRC code is attached to the input sequence. In the next step the input bit sequence to the code block segmentation is compared to the maximum code word size which is 6144 and if larger, the segmentation is performed and CRC is attached to each code block (CRC 24). Segmented code blocks are coded based on the channel coding scheme described in Chapter 8 (Channel Coding and Rate Matching). As mentioned before for data channels, a turbo coder with the rate of 1/3 is used. The rate matching block consists of three stages, a sub block interleaver (each code word is interleaved individually), bit collection, and then bit selection and puncturing. The last step is bit concatenation, which puts the rate matched code blocks together and generates the total number of coded bits for transmission [18].

Concatenated code word is scrambled before going through the modulation schemes. The maximum of two code words can be transmitted within the duration of one subframe. Scrambling of bits is based on 31-order Gold Code which is a simple modulo two

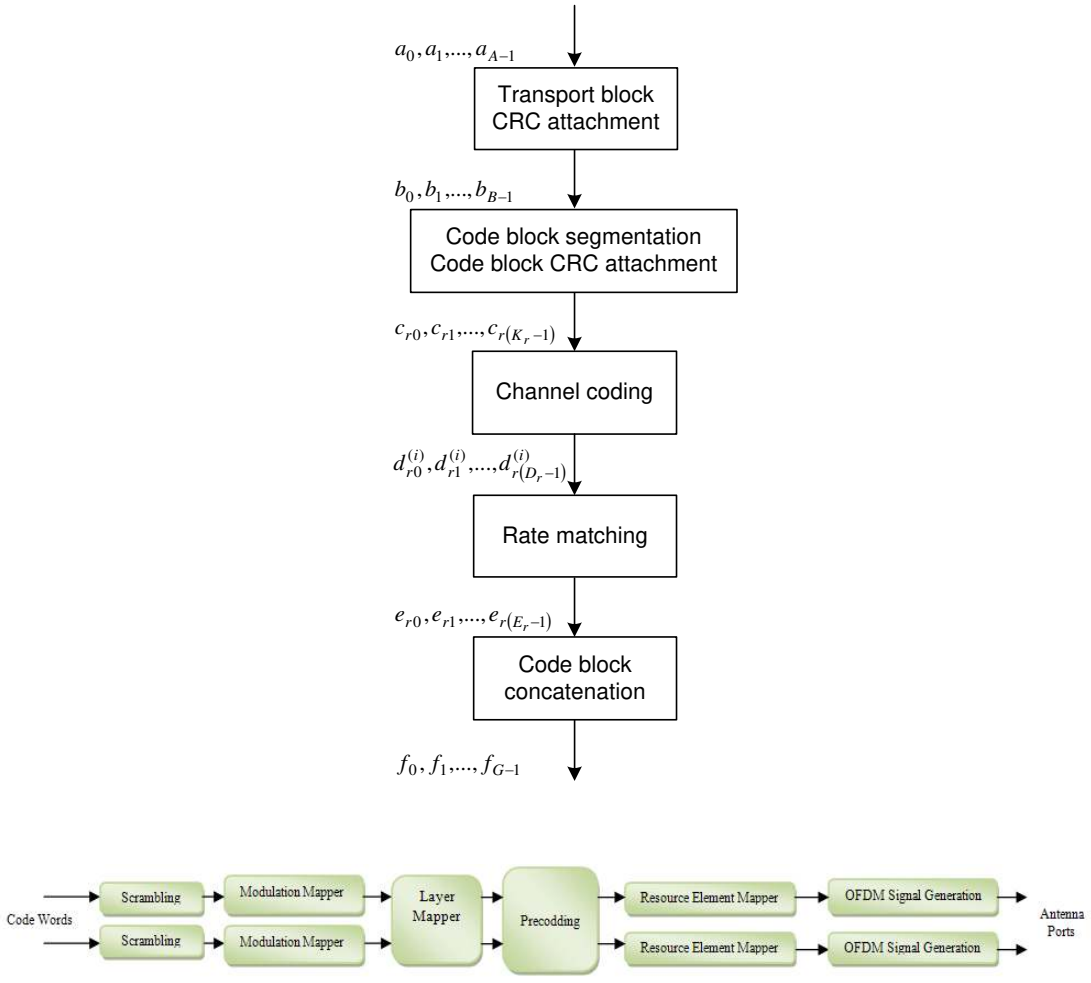

Figure 7.1 Downlink transport channel and physical channel processing for data transmission [3, 18]

addition of maximum two sequences. The modulation mapper modulates the scrambled bits with QPSK, 16QAM or, 64-QAM schemes and the layer mapper assigns the modulated symbols to layers depending on the number of antenna ports used for data transmission (1, 2 or 4 in case of downlink).

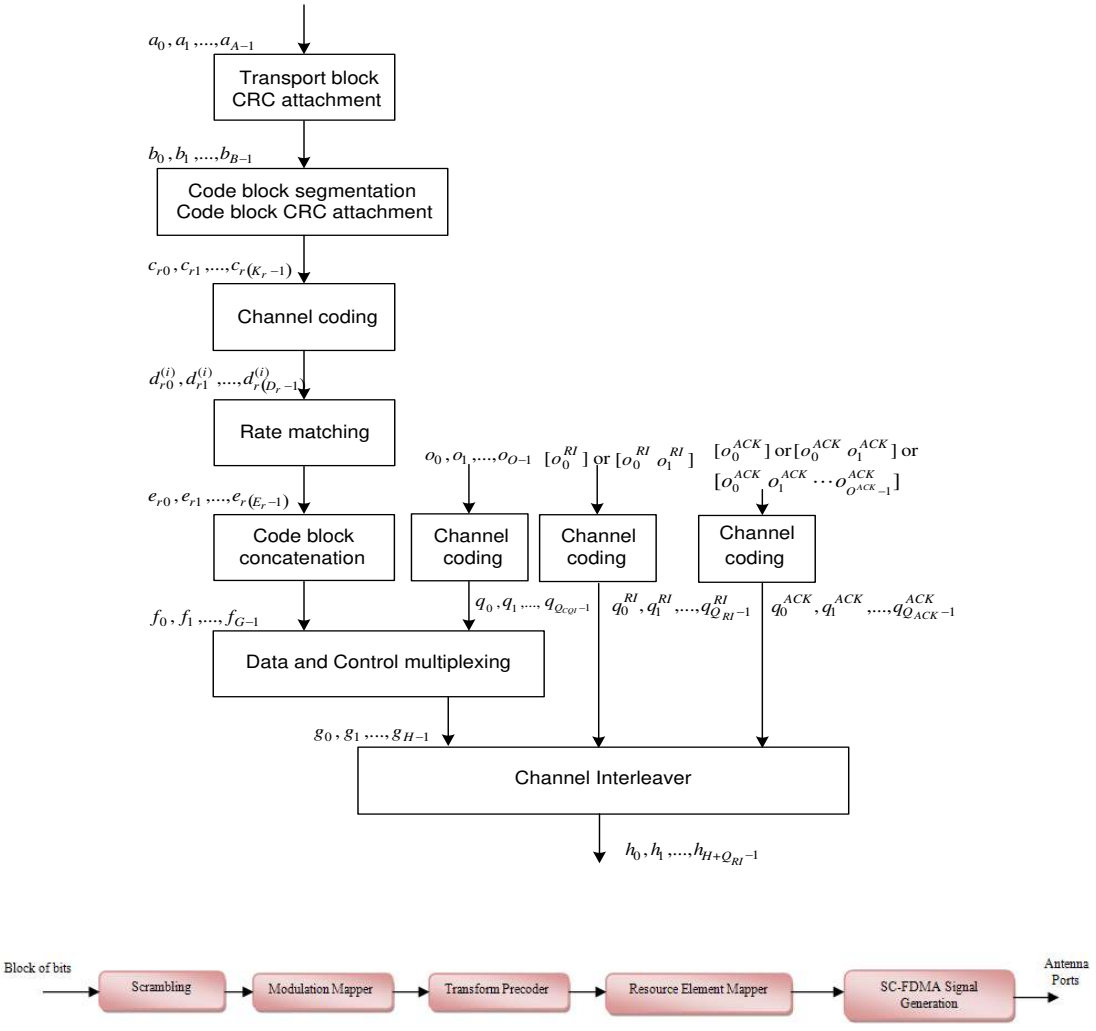

Figure 7.2 Uplink transport channel and physical channel processing for data transmission [3, 18]

The precoding step depends on the number of antenna ports and has different schemes for spatial multiplexing and transmits diversity. Mapping to the resource element is described in Chapter 7 (Physical Channels and Reference Signals) for downlink transmission and OFDM signal generation is described in Chapter 6 (Physical layer General Description).

Figure 7.2 illustrates the transport and physical channel processing for uplink transmission. The sequence of codeword generation is similar to what has been discussed about downlink transmission. After concatenation, the data and CQI or/and PMI control information are multiplexed together and followed by the channel interleaver. The procedure of this interleaver actually is to map the adjacent data symbols to the adjacent SC-FDMA symbols in the time domain first and then in the frequency domain (across the subcarriers). One of the steps for physical channel procedure that does not exist in downlink is the transform precoding. This procedure refers to dividing the block of input symbols M into M/ NSC_{rb} sets that each set corresponds to one SC-FDMA symbol.

For BER calculation, we need the downlink and uplink transport and physical channel processing implemented for both receiving and transmitting tracks. For this purpose, the Code Modulated Library (CML) is used to simulate the LTE physical layer procedure. This library is based on Matlab and C functions for implementing turbo coder, interleavers, rate matching, etc.

In the CML, the “LTEScenarios” Matlab function gets some of the parameters for simulation such as modulation scheme, codeword size, channel model, etc. the list of parameters and associated values are described in Chapter 8 (Results and Analysis).

Chapter 8. **Results and Analysis**

In this chapter the results of the simulation are illustrated and discussed. As mentioned in the Chapter 7 (modeling and Simulation), simulations are carried out with the minimum and maximum codeword sizes (40 and 6144). The channel mode is assumed to be AWGN and normal cyclic prefix is used. The LTE turbo code basic code rate is 1/3 and supported modulation schemes are QPSK, 16-QAM, and 64-QAM. Table 8.1 summarizes the simulation parameters.

Table 8.1 Simulation parameters

Parameter	Value(s)
Channel Bandwidth	1.4, 3, 5, 10, 15, 20 (MHz)
FFT Length	2048
Maximum Number of RBs	100
Duplex Mode	FDD, TDD
Channel Type	AWGN
FEC Coding Scheme	Turbo coding, R=1/3
Modulation	QPSK, 16-QAM, 64-QAM
Frame Period	10 ms
Subcarrier spacing	15 kHz
Cyclic prefix	Normal
Code Block Sizes	40, 6144
Code Rates	0.33 to 0.92
Antenna Diversity	SISO, 2x2 MIMO, and 4x4 MIMO
Maximum iteration of turbo code	10
Wrap up depth for turbo code	6
Min BER	10^{-9}
Max BER	10^{-4}
Number of Errors	300

Figure 8.1 demonstrates the BER values versus SNR respectively for QPSK, 16-QAM and 64-QAM modulation schemes for minimum and maximum codeword size. It is shown that the SNR gains for longer frame size is less than short frame sizes. Throughput calculations are based on the FER values that are applied to maximum and minimum codeword sizes.

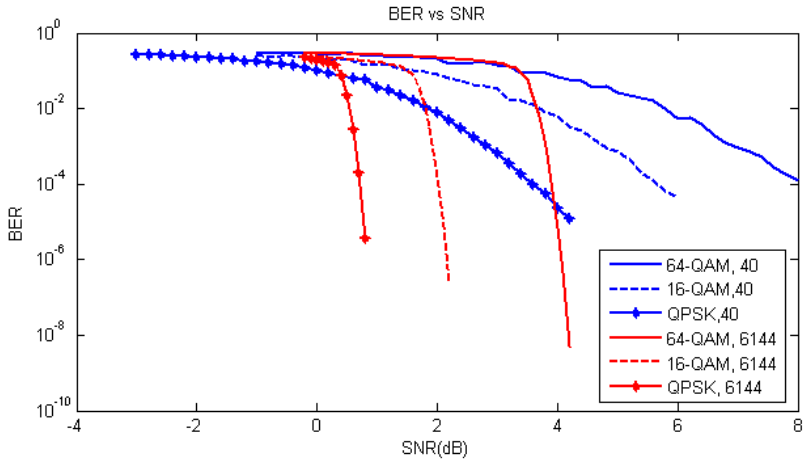

Figure 8.1 BER vs. SNR for QPSK, 16-QAM, and 64-QAM schemes

8.1 FDD Downlink Result Analysis

Figure 11.2 shows FDD downlink throughput in Mbps for one and four antenna ports and 1.4 MHz and 20MHz of system bandwidth in different modulation schemes. In these simulations, one OFDM symbol is assigned to PDCCH. The maximum throughput in 1.4 MHz of system bandwidth, one antenna port, two OFDM symbols assigned for PDCCH and 64-QAM modulation with 0.71code rate is 3.935 Mbps; in 20 MHz bandwidth, four antenna ports, 64-QAM data modulation, 276.32 Mbps of data throughput is possible. based on 0.84 puncture code rate; however, if this puncture code rate increases to the

maximum of 0.92 the throughput of 299.122 Mbps can be achieved. If we assume that there are two antenna ports used for downlink data transmission, considering the least resource elements assigned to control information (one OFDM symbol), 64-QAM data modulation, 0.92 puncturing code rate, and 20MHz system bandwidth, 158.366 Mbps of throughput is possible (maximum throughput in 2x2 antenna port scenario).

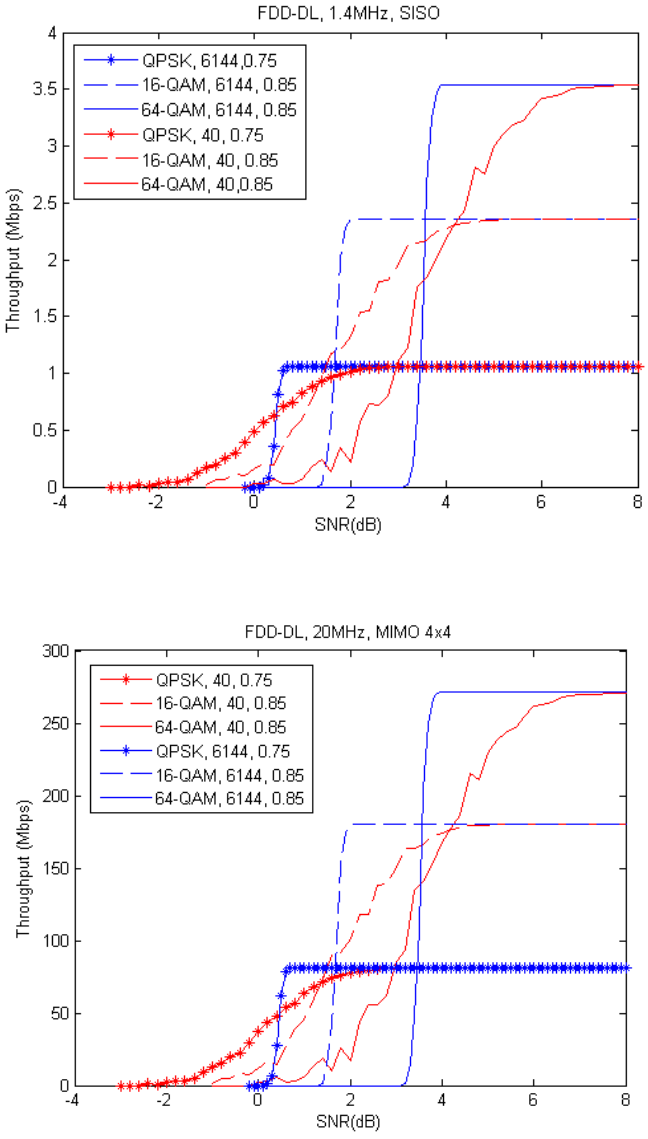

Figure 8.2 FDD PDSCH throughput

Therefore based on the resource elements that is proposed in Figures 6.1 to 6.3 of chapter 6 (proposed problem study), we can calculate the maximum throughput of different scenarios by applying the modulation scheme and puncturing code rate. These scenarios in FDD downlink can include different channel bandwidths (1.4, 3, 5, 10, 15, 20 MHz), antenna ports (1, 2, or 4), control channel overhead (1 to 4 OFDM symbols), and code rates (0.15 to 0.92). For example, based on Figure 6.7, in case of 15 MHz bandwidth, two antenna ports, and assigning two FDM symbol for PDCCH, the number of resource elements for PDSCH is 196896 in one radio frame. So applying the modulation schemes of 64-QAM, 16-QAM and QPSK with code rates 0.92, 0.85, 0.71 respectively, the throughput is 108.868 Mbps, 66.94 Mbps, and 27.959Mbps for each case.

Besides the throughput calculation, based on tables provided in section 5.3 (Physical Channels and Reference Signals), such as table 5.7 that provides the resource elements assigned for PDCCH in different antenna ports and bandwidths, we can calculate the overhead of each control channel or even reference signals. For instance in case of 20 MHz system bandwidth, and 4 antenna ports, the PDCCH overhead is 1.06 Mbps, 4.26 Mbps, 7.46 Mbps for 1,2 and 3 OFDM symbols assigned to this channel and considering that the modulation is QPSK for this channel and the code rate is 1/3. This calculation excludes PCFICH that occupies 16 OFDM resource elements of the first OFDM symbol since the code rate for this channel is 1/6. So for the maximum data throughput of 299.122 Mbps, PDCCH overhead is 1.06 Mbps which is 2.37% of the total physical layer.

8.2 FDD Uplink Result Analysis

Figure 8.3 illustrates throughput simulation results for uplink transmission. Considering the maximum bandwidth and 64-QAM modulation, the maximum PUSCH throughput is 71.97 Mbps by applying 0.85 puncture code rate.

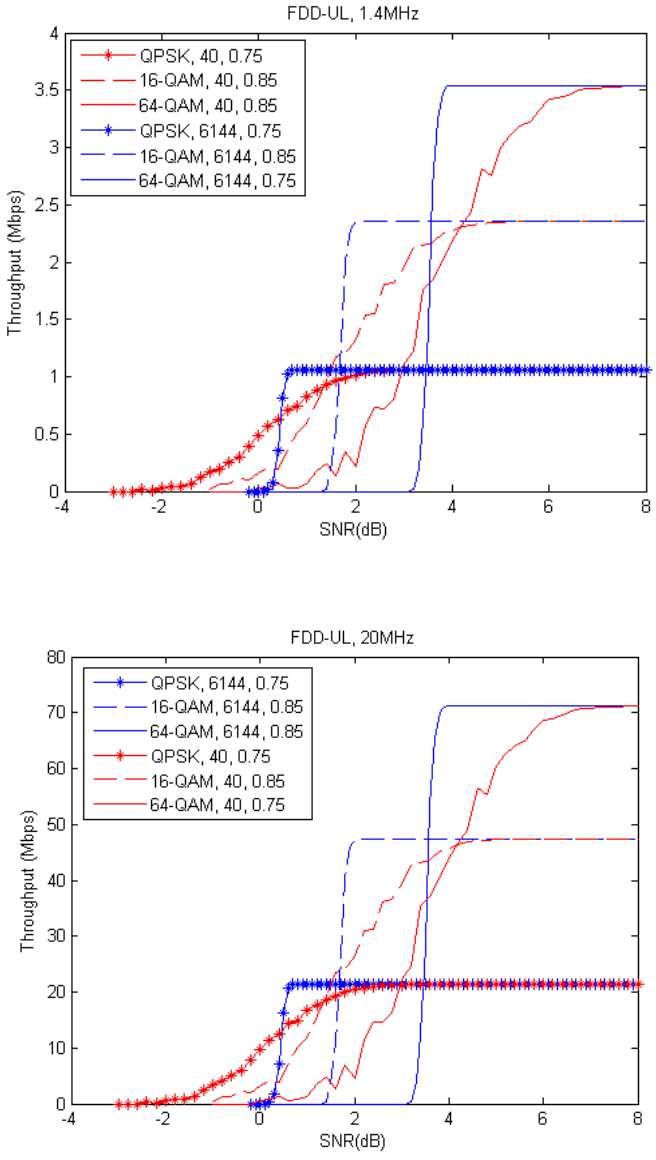

Figure 8.3 FDD PUSCH throughput

Due to the fact that in LTE Release 8 there can be two antennas in Uplink but the MIMO technique is the close loop rank 1. In this technique only one antenna port is available for data transmission, therefore physical layer has the capacity of two antennas however just one antenna in used at a time. So the throughput is calculated based on one antenna transmission. In later release of LTE (Release 10) both antenna ports are available for data transmission. Creating different scenarios is possible in uplink too, based on different bandwidths, modulation schemes, and code rates. For example in case of 15 MHz channel bandwidth in uplink, the maximum resource elements assigned for PUSCH is 105120 in one radio frame. Hence the throughput for uplink data is 53.612 Mbps, 35.74 Mbps, and 14.92 in case of 64-QAM with 0.85 code rate, 16-QAM with 0.85 code rate, and QPSK with 0.71 code rate.

The overhead calculation for control channels and reference signals in uplink is possible as well as downlink, based on the information provided in section 5.3 (Physical Layers and Reference Signals) since the resource elements allotted for control channel and reference signals is given in this chapter. For example assuming 2/2a/2b format for PUCCH, the number of resource elements assigned to this channel is 2880 in all the bandwidths excluding demodulation reference signal associated with this channel. (PUCCH is mapped to the sided resource blocks of the overall bandwidth). Therefore, the overhead of PUCCH is 0.192 Mbps. In case of the maximum throughput of PUSCH, which is 71.97 Mbps, the overhead for PUCCH is 1.71% of the uplink physical channel.

8.3 TDD Downlink and Uplink Result Analysis

Figures 8.4 and 8.5 show PDSCH and PUSCH throughput results, respectively, considering mode 0 (labeled as M0) and mode 5 (labeled as M5) of TDD configuration.

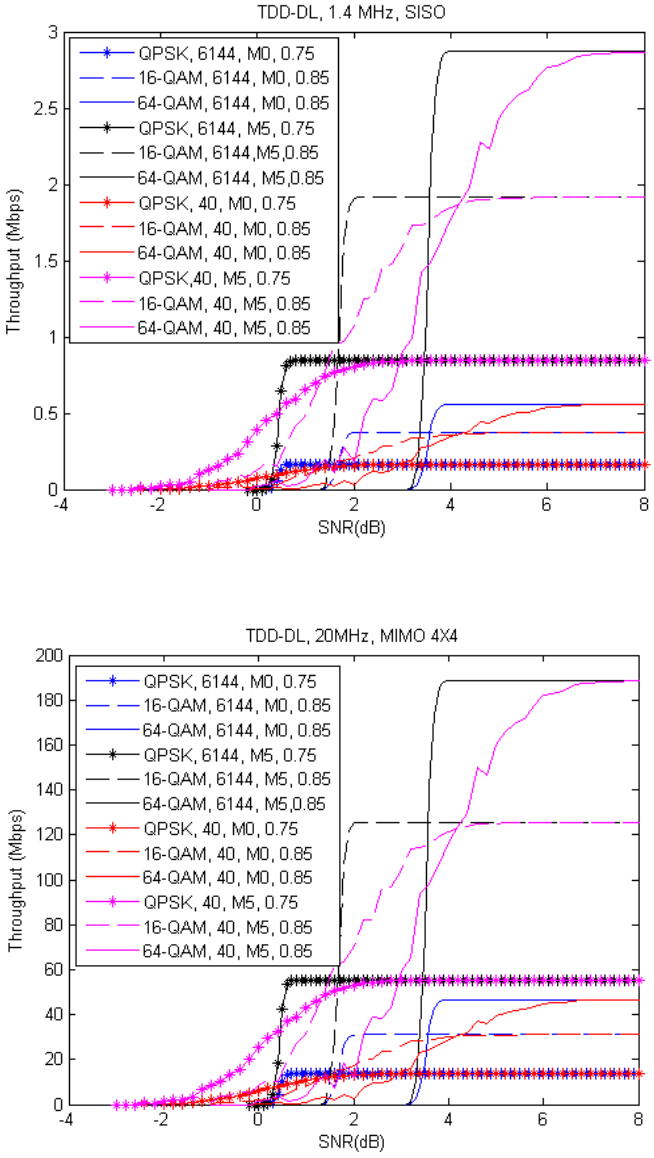

Figure 8.4 TDD PDSCH throughput

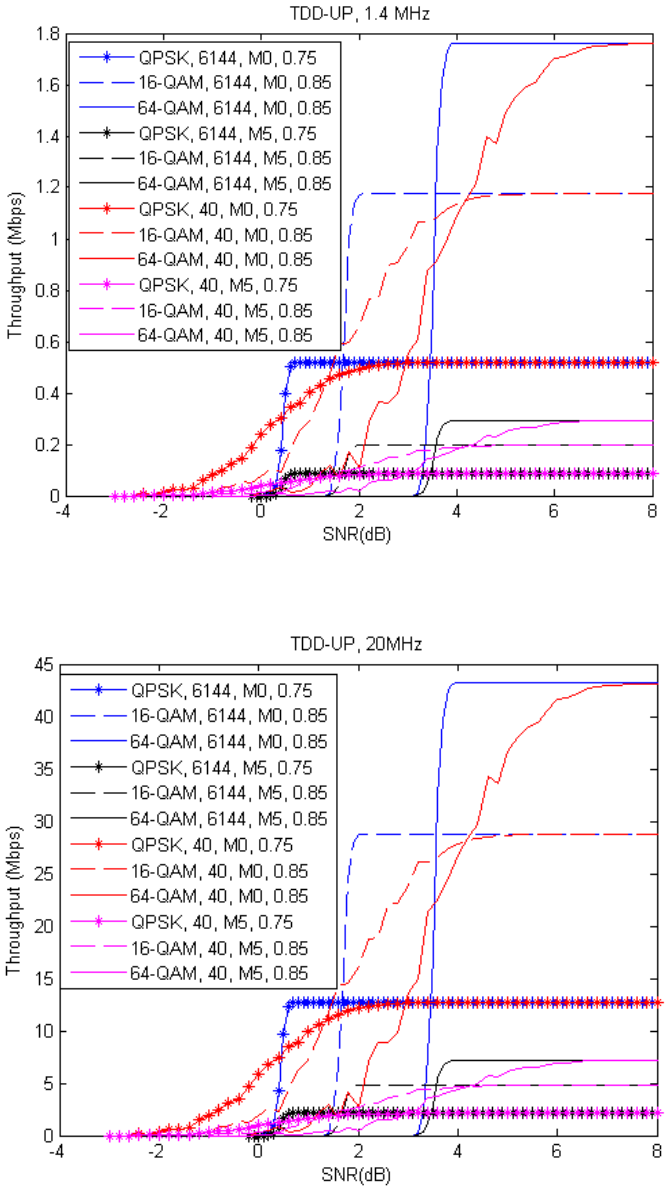

Figure 8.5 TDD PUSCH throughput

Throughput calculation in these two figures is based on 1.4 and 20 MHz channel bandwidth, employing QPSK, 16-QAM, and 64-QAM, 0.71 and 0.85 puncture code rate, and one four antenna ports in downlink. Figure 8.4 illustrates that the maximum

throughput of PDSCH in mode 0 is 48.630 Mbps since only two subframes are available for downlink transmission. However, in mode 5, which carries downlink information in eight subframes, this value improves to 205.684 Mbps. For throughput calculation of PDSCH in TDD operation, it is assumed that 3 OFDM symbols are assigned for PDCCH; hence the throughput will be improved by assuming less overhead for control channel. PUSCH occupies six subframes for data transmissions in Mode 0, providing 42.696 Mbps as the maximum PUSCH throughput (64-QAM modulation, 0.85 code rate, and 20MHz bandwidth) as shown in Figure 8.5. In Mode5, which uses one subframe for Uplink transmission, 7.116 Mbps of throughput is feasible.

The Overhead for TDD operation can be calculated similarly to FDD; however in TDD operation the special subframe contains Guard Period and uplink pilot overhead too. The overhead of guard period and uplink pilot based on the switch point periodicity is different due to the fact that in 5 ms switch point periodicity, there are two special subframes in a radio frame, but in 10 ms switch point periodicity, only one special subframe consists in a radio frame.

Chapter 9. **Summary and Conclusions**

9.1 Summary

Evolution of wireless communication has been expanded in recent years by introducing the 3rd generation of standards. This evolution is based on demands for higher data rate, lower latency, and better coverage resulting in user satisfaction. LTE Release 8 provides high peak data rates of 300 Mbps on the downlink and 75 Mbps on uplink for 20 MHZ bandwidth. In this study, the maximum throughput of downlink and uplink transmission is investigated depending on different scenarios for the physical layer.

In this study the throughput calculation exclusively contains data channels (PUSCH and PDSCH) for both FDD and TDD operations. For throughput analysis, different resource elements that are assigned for data channels of downlink and uplink are calculated for FDD and TDD operations in different conditions. FDD downlink resource elements are calculated for all the possible system bandwidths (1.4 MHz to 20 MHz) and antenna ports (1,2 and 4 antenna ports). These results are presented in chapter 9 (Proposed Performance Study).

In chapter 8 (results and analysis), by using the results from chapter 5 (proposed performance study), throughput is illustrated versus SNR gains based on FER values gained from the link level simulation. The procedure of link level simulation is outlined

in chapter 7 (modeling and simulating) that uses CML library on MATLAB for implementing the simulation procedure.

Results show that the maximum data throughput is 299.122 Mbps for downlink (assuming 4 antenna ports, 64-QAM modulation, one OFDM symbol assigned for PDCCH, 0.92 code rate, and 20MHz system bandwidth) and 71.97 Mbps for uplink (assuming 64-QAM modulation, 0.85 code rate, and 20MHz system bandwidth), excluding all control and reference signal information overhead in FDD operation.

In TDD operation the maximum throughput of downlink data channel is 205.684 Mbps which is achieved in mode 5 of TDD frame configurations. This calculation is based on, 64-QAM modulation, 0.85 code rate, 4 antenna ports, 3 PDCCH OFDM symbols, and 20 MHz system bandwidth. however the maximum throughput for uplink data is 42.696 Mbps assuming 64-QAM modulation, 0.85 coderate, and 20 MHz bandwidth.

Simulation results show high performance in respect to signal- to-noise ratio gains which is resulted from turbo coding, interleaver and rate matching algorithm. This performance is achieved based on specific parameters discussed in Chapter 7 (Modeling and Simulation) and Chapter 8 (Results and Analysis) such as number of iterations, wrap up depth for constituent convolutional encoder in the turbo encoder.

9.2 Conclusions

This study consists of comprehensive analysis of LTE Release 8 performance based on different scenarios. According to what is discussed in chapter 4 (Literature Review), previous studies are not complete and does not discuss all of the possible scenarios such as different operation schemes (FDD and TDD), possible antenna diversity schemes (1, 2, and 4 in downlink), data channels in both uplink and downlink, different system bandwidths, and code rates. Furthermore, the maximum throughput calculation still includes control and reference signal information.

In this investigation, the throughput calculation includes both FDD and TDD for uplink and downlink. Moreover the impact of different antenna ports in downlink is presented as well as different overhead possible for control channel. Moreover, the throughput analysis is exclusively related to data channels (PUSCH And PDSCH) and does not include the information of control channels and reference signal.

This research can be expanded to address the maximum throughput and overhead of upper layers such as MAC and RLC. Different structures and configurations of MAC PDUs can also be studied. Moreover, due to the evolution track toward 4G wireless communication standards, evaluation of physical layer throughput can be performed for Release 10 3GPP since new technologies such as bandwidth extension up to 100MHz via carrier aggregation and supporting more antenna ports (8 in downlink and 4 in uplink) can highly influence performance.

References

[1]. Wireless Communications: Principles and Practice, Theodorse, S.Rappaport, Prentice-Hall, 2nd, 2002, ISBN 0-13-042232-0.

[2]. NGMN, 'Next Generation Mobile Networks beyond HSPA & EVDO – A white paper', www.ngmn.org, December 2006.

[3]. 3GPP TS 36.300, "Evolved Universal Terrestrial Radio Access (EUTRA); Overall Description" (Release 8)

[4]. 3GPP TS 23.402, UTRAN- and E-UTRAN-based systems "Architecture enhancement for non-3GPP access" (Release 8)

[5]. 3GPP TS 23.401, E-UTRAN-based systems, "General Packet Radio Service (GPRS) enhancements for Evolved Universal Terrestrial Radio Access Network (E-UTRAN) access" (Release 8)

[6]. 3GPP TS 36.211, "Evolved Universal Terrestrial Radio Access (EUTRA); physical channels and modulations" (Release 8)

[7]. D. Astély, E. Dahlman, A. Furuskär, Y. Jading, M. Lindström, and S. Parkvall, "LTE: the evolution of mobile broadband", IEEE communication magazine, April 2009.

[8]. A. Larmo, M. Lindström, M. Meyer, G. Pelletier, Johan Torsner, H. Wiemann, "The LTE link-layer design", IEEE Communications Magazine, v.47 n.4, p.52-59, April 2009.

[9]. J. J. Sánchez, D. Morales-Jiménez, G. Gómez, J. T. Enbrambasaguas, "Physical Layer Performance of Long Term Evolution Cellular Technology", 16th IST Mobile and Wireless Communications Summit, 2007.

[10]. C. Ball, T. Hindelang, I. Kambourov, S. Eder, "Spectral Efficiency Assessment and Radio Performance Comparison between LTE and WiMAX ", 2008 IEEE

[11]. A. Furuskär, T. Jönsson, M. Lundevall Ericsson Research, Sweden, "The LTE Radio Interface- key Characteristics and Performance" Personal, Indoor and Mobile Radio Communications, September 2008 IEEE

[12]. J. lee, j. han, j. zhang, "MIMO technologies in 3GPP LTE and LTE-Advanced," journal on wireless communications and networking, 2009.

[13]. Y. Yang, H. Hu, J. Xu, G. Mao, "Relay Technologies for WiMAX and LTE-Advanced Mobile Systems", Communications Magazine, IEEE, Vol. 47, No. 10. (02 October 2009), pp. 100-105.

[14]. E. Virtej, M. Kuusela, E. Tuomaala, "System Performance of Single-User MIMO in LTE Downlink", Personal, Indoor and Mobile Radio Communications, 2008. PIMRC 2008. IEEE 19th International Symposium on, September 2008

[15]. PMogensen , W. Na, I. Z. Kovács, F. Frederiksen, A. Pokhariyal, K. I. Pedersen, T. Kolding, K. Hugl, M. Kuusela, "LTE Capacity compared to the Shannon Bound", IEEE 65th Vehicular Technology Conference VTC, January 2007

[16]. freescale semiconductor "Long Term Evolution Protocol Overview" white paper, October 2008

[17]. J. Zyren, W. McCoy, "Overview of the 3GPP Long Term Evolution Physical Layer", white paper by freescale semiconductor, June 2007.

[18]. 3GPP TS 36.212 "Evolved Universal Terrestrial Radio Access (EUTRA); physical channels and modulations", Multiplexing and Channel Coding (Release 8)

[19]. 3GPP TS 36.213, "Evolved Universal Terrestrial Radio Access (EUTRA); physical channels and modulations", Physical layer procedure (Release 8)

[20]. D. M. Sacristán, J. Cabrejas, D. Calabuig, J. F. Monserrat , Institute of Telecommunications and Multimedia Applications, "MAC Layer Performance of Different Channel Estimation Techniques in UTRAN LTE Downlink", 69th Vehicular Technology Conference (VTC) IEEE, June 2009

[21]. D.M. Sacristán, J. F. Monserrat, J. Cabrejas, D. Calabuig, S. Garrigas, N. Cardona, " On the Way towards Fourth-Generation Mobile: 3GPP LTE and LTE-Advanced ", EURASIP Journal on Wireless Communications and Networking, July 2009

[22]. 3GPP R1-072261, "LTE Performance Evaluation—Uplink Summary," May 2007.

[23]. 3GPP R1-072578, "Summary of Downlink Performance Evaluation," May 2007.

[24]. Q. Li, G. Li, W. Lee and M. Lee, D. Mazzarese, B. Clerckx, S. Z. Li, "MIMO Techniques in WiMAX and LTE: A Feature Overview", IEEE communication Magazine, May 2010.

[25]. A. Ghosh, R. Ratasuk, B. Mondal, N. Mangalvedhe, T. Thomas, "LTE-Advanced: next-generation wireless broadband technology", IEEE Wireless Communication, June 2010.

[26]. M. Iwamura, K. Etemad, M.H. Fong, R. Nory, R. Love, "Carrier Aggregation Framework in 3GPP LTE-Advanced", IEEE communication Magazine, August 2010.

[27]. K. Kusume, G. Dietl, T. Abe, H. Taoka, S. Nagata, "System Level Performance of Downlink MU-MIMO Transmission for 3GPP LTE-Advanced", Vehicular Technology Conference (VTC), IEEE 71st , june 2010.

[28]. S. Sesia , I. Toufik, M. Baker,"LTE The UMTS Long Term Evolution from theory to practice", 2009 John Wiley & Sons Ltd.

[29]. F. Rezaei, M. Hempel, H. Sharif, "LTE PHY Performance Analysis under strict 3GPP parameters", submitted to Vehicular Technology Conference (VTC) September 2010.

[30]. J.F. Cheng, A. Nimbalker, Y. Blankenship, B. Classon, T. K. Blankenship, "Analysis of Circular Buffer Rate Matching for LTE Turbo Code" Vehicular Technology Conference (VTC) IEEE 68th, September 2008.

[31]. 3GPP TS 23.331, UTRAN- and E-UTRAN-based systems "Radio Resource Control Protocol Specification" (Release 8)

[32]. 3GPP TS 23.323, UTRAN- and E-UTRAN-based systems "Packet Data Coverage Protocol Specification" (Release 8)

[33]. 3GPP TS 23.322, UTRAN- and E-UTRAN-based systems "Radio Link Control Protocol Specification" (Release 8)

[34]. 3GPP TS 23.321, UTRAN- and E-UTRAN-based systems "Medium Access Control Protocol Specification" (Release 8)

[35]. 3GPP TS 36.101, UTRAN- and E-UTRAN-based systems "User Equipment (UE) Radio Transmission and Reception" (Release 8)

[36]. 3GPP TS 36.104, UTRAN- and E-UTRAN-based systems "Base Station Radio Transmission and Reception" (Release 8)

[37]. 3GPP TS 36.302, UTRAN- and E-UTRAN-based systems "Services provided by the physical layer" (Release 8)

[38]. 3GPP TS 36.412, UTRAN- and E-UTRAN-based systems "Services provided by the physical layer" (Release 8)

[39]. 3GPP TS 36.412, UTRAN- and E-UTRAN-based systems "x2 general aspects and principals" (Release 8)